

Symmetry Properties of Quantum Dynamical Entropy

Eric D. Schultz,^a Keiichiro Furuya^b and Laimei Nie^a

^a*Department of Physics and Astronomy, Purdue University,
West Lafayette, IN 47907, U.S.A.*

^b*Department of Physics, Northeastern University,
Boston, MA 02115, U.S.A.*

E-mail: schul211@purdue.edu, k.furuya@northeastern.edu, nlm@purdue.edu

ABSTRACT: We investigate the relation between the Alicki-Fannes-Lindblad (AFL) quantum dynamical entropy and quantum symmetries. We show that, while the cumulative AFL entropy generally saturates to the dimensional bound at late times for chaotic dynamics, this saturation value is distinctively lower when the partitions (measurements) respect the symmetries. We provide rigorous analysis to this lowered value in three cases: Abelian symmetries, anticommuting unitaries, and non-Abelian symmetries. We further support our analytical results with numerical simulations of the perturbed quantum cat maps. Our findings highlight the complex relationship between the cumulative AFL entropy and symmetries, and suggest that caution is needed when interpreting it as an indicator of quantum chaos.

Contents

1	Introduction	2
2	Alicki-Fannes-Lindblad Entropy	3
2.1	Definitions	3
2.2	AFL entropy in Finite Dimensions	5
3	Cumulative AFL in Quantum Cat Map: Numerics	6
3.1	The Quantum Cat Map and its Symmetries	6
3.2	Cumulative AFL in Quantum Cat Map	7
4	Abelian Symmetry	10
4.1	Theorem 1	11
4.2	Proof of Theorem 1	12
5	Tensor Product Dynamics	13
5.1	Theorem 2	14
5.2	Anticommuting Unitary	14
5.3	Proof of Theorem 2	15
6	Non-Abelian Symmetries	16
7	Discussions	18
7.1	Types of Quantum Chaos	19
7.2	Relation to CNT Entropy	19
A	The Cat Map	19
A.1	Classical Cat Map	19
A.2	Quantizing the Cat Map	20
A.3	Proof of Anticommutation	21
A.4	The R and W Algebra	23
B	Proof of Theorem 1 in System and Purifier Space	27

1 Introduction

In classical dynamical systems, the Kolmogorov-Sinai (KS) serves as a key indicator of chaos [1]. It is defined as the maximum asymptotic rate at which information about the system's state is gained by making successive measurements. To compute the KS entropy, one typically partitions the phase space into distinct cells. These partitions are observations needed to track the system's evolution. By overlaying the time-evolved partitions from successive time steps, an increasingly fine-grained composite partition is created that captures the spreading of trajectories across the phase space. The KS entropy, defined as the growth rate of the Shannon entropy of the composite partition, essentially measures the exponential divergence of initially nearby trajectories.

Quantum dynamical entropies are generalizations of the classical KS entropy to non-commutative (quantum) dynamical systems. Various quantum dynamical entropies have been proposed with the goal of elucidating quantum chaos, including [2–11]. Among these, the Alicki-Fannes-Lindblad (AFL) entropy, which employs finite operational partitions of unity, has proven particularly useful for characterizing quantum chaos, bounding classical channel capacities, and analyzing the spacio-temporal structure of quantum information [4, 12–16]. Another prominent example is the Connes-Narnhofer-Thirring (CNT) entropy, whose construction involves a set of completely positive maps between C^* -algebras [2, 3].

While quantum dynamical entropies have been extensively studied, their properties under quantum symmetries remain largely unexplored. In general, symmetries play a crucial role in quantum dynamics [17–23]. In the presence of symmetries, dynamics is constrained to the superselection sectors, leading to changes in the behavior of chaos measures such as level statistics and out-of-time-ordered correlator [18, 19, 24].

This work investigates the impact of symmetries specifically on AFL entropy. For finite size quantum systems, where typical AFL entropy vanishes due to limited Hilbert space capacity, the cumulative AFL entropy provides a more meaningful measure. It typically exhibits an initial Lyapunov growth phase, followed by saturation at a value determined by the system's dimension, assuming complex and chaotic dynamics. Our key finding is that when partitions (measurements) respect the symmetries of the dynamics, the late-time saturation value of the cumulative AFL entropy is reduced. We provide rigorous analysis that explains precisely this lowered value in three cases: Abelian symmetries, anticommuting unitaries, and non-Abelian symmetries. Conversely, symmetry-incompatible partitions lead to the cumulative AFL entropy saturating to the usual dimensional bound, effectively masking the presence of symmetries.

Our study was motivated by numerical observations in quantum cat map, a paradigmatic model for the study of quantum chaos (see [25–28] for some recent work). Its well-understood structure and tunable symmetries make them an ideal playground for exploring how symmetries influence AFL entropy.

This paper is organized as follows. Section 2 introduces the construction of (cumulative) AFL entropy, with an emphasis on finite dimensional systems. Section 3 presents numerical evidence of cumulative AFL entropy in quantum cat maps with various types

of symmetries. We then provide analytical explanations to the numerical observations in Sections 4, 5 and 6. Further discussions regarding (cumulative) AFL entropy's potential as a quantum chaos indicator, as well as its relation with other quantum dynamical entropies, can be found in Section 7.

2 Alicki-Fannes-Lindblad Entropy

2.1 Definitions

The construction of AFL entropy is due to Alicki and Fannes [4] based on earlier work by Lindblad [29, 30], and is analogous to that of KS entropy (see also [12–15]). The system S is governed by a discrete unitary dynamics U and a density matrix ρ on an N -dimensional Hilbert space \mathcal{H}_S . The state ρ is analogous to the measure in classical dynamical systems, and is similarly required to be stationary: $[U, \rho] = 0$. A generalized measurement on the system may be represented with Kraus operators $\mathcal{X} = \{X^1, \dots, X^K\}$ with $\sum_i X^{i\dagger} X^i = \mathbb{1}$ [31, 32]. The measurement channel (without post-selection) $\mathcal{E}_{\mathcal{X}}$ acts as $\mathcal{E}_{\mathcal{X}}(\rho) = \sum_i X^i \rho X^{i\dagger}$. In analogy to the phase-space partition of KS entropy, \mathcal{X} is referred to as an *operational partition of unity* (or simply a *partition*) of size K .

Entropy exchange. The measurement channel may be written as a unitary process on an enlarged Hilbert space including the environment (measurement device). In this view, the channel generates entanglement between the system and environment known as entropy exchange [30, 33]. To discount the entanglement entropy present in ρ prior to the channel, we purify the state by introducing a purifier P with Hilbert space \mathcal{H}_P isomorphic to \mathcal{H}_S . Diagonalizing the density matrix as $\rho = \sum_{\alpha} r_{\alpha} |\psi_{\alpha}\rangle\langle\psi_{\alpha}|$, a canonical purification is $|\sqrt{\rho}\rangle\rangle = \sum_{\alpha} \sqrt{r_{\alpha}} |\psi_{\alpha}\rangle|\psi_{\alpha}\rangle$, which lives in the doubled Hilbert space $\mathcal{H}_S \otimes \mathcal{H}_P$. Here, $|\cdot\rangle\rangle$ notates the Choi state of an operator with respect to the eigenbasis of ρ , given by $|\mathcal{O}\rangle\rangle = \sum_{\alpha\beta} \mathcal{O}_{\alpha\beta} |\psi_{\alpha}\rangle|\psi_{\beta}\rangle$ for an operator \mathcal{O} on \mathcal{H}_S [32].

Given a partition of size K , the measurement outcomes correspond to orthogonal states $|1\rangle, \dots, |K\rangle$ in the environment E with Hilbert space \mathcal{H}_E . Dilating the channel to a unitary process on $\mathcal{H}_E \otimes \mathcal{H}_S \otimes \mathcal{H}_P$, a measurement maps

$$|1\rangle|\sqrt{\rho}\rangle\rangle \mapsto \sum_{i=1}^K |i\rangle|X^i\sqrt{\rho}\rangle\rangle =: |\Psi\rangle \quad (2.1)$$

which one may check is normalized. Tracing out SP , the state of the environment is

$$\tilde{\rho}[\mathcal{X}] = \text{Tr}_{SP} |\Psi\rangle\langle\Psi| = \sum_{ij} \text{Tr}(X^i \rho X^{j\dagger}) |i\rangle\langle j|. \quad (2.2)$$

The *entropy exchange* is defined as the entanglement with the environment generated by the measurement. More precisely, it is the von Neumann entropy of $\tilde{\rho}[\mathcal{X}]$,

$$S(\tilde{\rho}[\mathcal{X}]) = -\text{Tr}(\tilde{\rho}[\mathcal{X}] \log \tilde{\rho}[\mathcal{X}]), \quad (2.3)$$

which may be equivalently computed by tracing out E to get the state on SP [12]

$$\sigma[\mathcal{X}] = \text{Tr}_E |\Psi\rangle\langle\Psi| = \sum_i |X^i\sqrt{\rho}\rangle\rangle\langle\langle X^i\sqrt{\rho}|, \quad (2.4)$$

$$S(\sigma[\mathcal{X}]) = -\text{Tr}(\sigma[\mathcal{X}] \log \sigma[\mathcal{X}]) = S(\tilde{\rho}[\mathcal{X}]) \quad (2.5)$$

since the state on ESP is pure. Both constructions are shown graphically in Fig. 1.

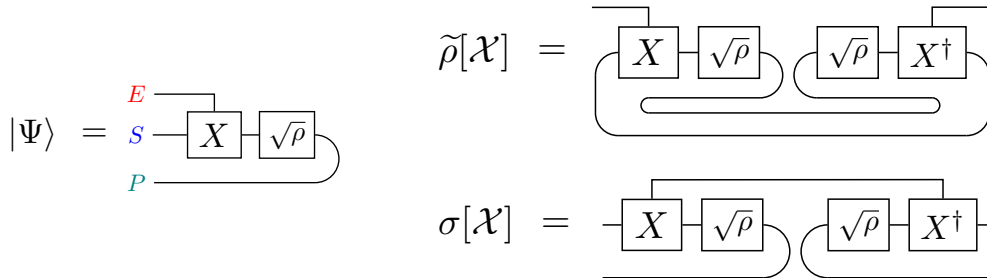


Figure 1: Tensor network representations of $|\Psi\rangle$, $\tilde{\rho}[\mathcal{X}]$, and $\sigma[\mathcal{X}]$. These are the pure state on ESP and the reduced states on E and SP respectively. The top line of X is the Kraus index, which is the environment Hilbert space \mathcal{H}_E . See [16] for further diagrams and [34, 35] for details on this notation more generally.

AFL entropy. In analogy with KS entropy, AFL entropy is the maximum rate of entropy production from periodic measurements. This means we apply the measurement channel (2.1) after each discrete evolution U . The graphical representation easily incorporates multiple time steps as shown in Fig. 2. This is equivalent to acting with a time-evolved partition, which we notate after t time steps as

$$(U\mathcal{X})^t := \{ UX^{i_t} \dots UX^{i_2} UX^{i_1} \mid i_j = 1, \dots, K \}. \quad (2.6)$$

The *cumulative AFL entropy* is defined as the entropy exchange of this multitime measurement channel:

$$H_{\text{AFL}}(\rho, U, \mathcal{X}, t) = S(\tilde{\rho}[(U\mathcal{X})^t]) = S(\sigma[(U\mathcal{X})^t]). \quad (2.7)$$

The *AFL entropy*, as with the classical KS entropy, is defined as the asymptotic growth rate of H_{AFL} maximized over all partitions:

$$h_{\text{AFL}}(\rho, U) = \sup_{\mathcal{X}} \limsup_{t \rightarrow \infty} \frac{1}{t} H_{\text{AFL}}(\rho, U, \mathcal{X}, t). \quad (2.8)$$

This definition is readily generalized to C^* -algebras, including infinite-dimensional quantum systems and classical dynamical systems. In the classical case, AFL entropy coincides with KS entropy [36, 37].

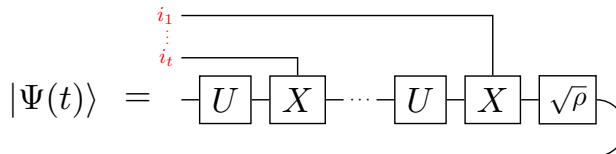


Figure 2: Tensor network representation of the pure state $|\Psi\rangle$ after t time steps.

2.2 AFL entropy in Finite Dimensions

Cumulative AFL entropy, as the entanglement entropy of a subsystem of a pure state, is dimensionally bounded [15]. The first dimensional bound comes from the environment. The dimension of \mathcal{H}_E at time t is at most K^t , so

$$H_{\text{AFL}}(\rho, U, \mathcal{X}, t) \leq t \log K \quad (2.9)$$

The complementary bound comes from system and purifier. Further traces of $\sigma[\mathcal{X}]$ give

$$\begin{aligned} \text{Tr}_S(\sigma[\mathcal{X}]) &= \rho \\ \text{Tr}_P(\sigma[\mathcal{X}]) &= \mathcal{E}_{\mathcal{X}}(\rho) \end{aligned} \quad (2.10)$$

as expected. By subadditivity of von Neumann entropy, the cumulative AFL entropy then obeys

$$\begin{aligned} H_{\text{AFL}}(\rho, U, \mathcal{X}, t) &= S(\sigma[(U\mathcal{X})^t]) \\ &\leq S(\rho) + S(\mathcal{E}_{(U\mathcal{X})^t}(\rho)) \\ &\leq S(\rho) + \log N \\ &\leq 2 \log N \end{aligned} \quad (2.11)$$

The cumulative AFL entropy is bounded above by a finite constant, and so the asymptotic growth must vanish: $h_{\text{AFL}}(\rho, U) = 0$ for all dynamics U on \mathcal{H}_S .

From this property, AFL entropy h_{AFL} is fundamentally ill-suited for studying quantum chaos in finite dimensions. The cumulative AFL entropy H_{AFL} , on the other hand, has been proposed as a possible alternative, potentially offering insight beyond the vanishing limit of equation (2.8). In practice, H_{AFL} is typically evaluated numerically. This involves selecting an initial state ρ and partition \mathcal{X} , and then tracking the density matrix of the SP space, $\sigma[(U\mathcal{X})^t]$. The advantage of using $\sigma[(U\mathcal{X})^t]$ instead of $\tilde{\rho}[(U\mathcal{X})^t]$ is that the former maintains a constant size over time.

Several studies have examined the behavior of H_{AFL} in various models. In the quantum kicked top and quantum baker’s map, numerics have indicated that cumulative AFL can identify the presence or absence of semiclassical chaos through, for example, early time¹ H_{AFL} ’s growth rate matching the corresponding classical Lyapunov exponent [12, 15]. This matching has been proved rigorously in the infinite-dimensional limit of the quantum cat map [38]. The cumulative AFL entropy was also studied on free fermions and SYK under the name “spacetime entropy” [16]. Despite these initial promising observations, the suitability of H_{AFL} for diagnosing quantum chaos, especially in finite dimensions, remains an open question. We address this gap by focusing on the influence of symmetries, which impose significant constraints on the quantum dynamics. In particular, we will show that the effectiveness of H_{AFL} strongly depends on the choice of partitions. When partitions are chosen to be compatible with a system’s symmetries, the growth of H_{AFL} is limited, saturating at a lower value. However, as shown in the next section, in practice the challenge

¹Early time refers to times prior to the semiclassical Ehrenfest time $t_E \sim |\log(\hbar)|/h_{\text{KS}}$ where h_{KS} is the Kolmogorov-Sinai entropy of the dynamics [15, 38, 39].

lies in identifying these symmetries a priori, as their absence can lead to H_{AFL} saturation that mimics fully chaotic dynamics.

3 Cumulative AFL in Quantum Cat Map: Numerics

3.1 The Quantum Cat Map and its Symmetries

Here, we present numerics showcasing the behaviors of cumulative AFL entropy in perturbed quantum cat maps, a well-studied family of single particle models. The unitary dynamics is derived from a discrete classical map on torus \mathbb{T}^2 , the Arnol'd cat map [40]. For more information on this map and its quantization, see Appx. A and references therein. In our work, we choose the perturbed cat map

$$\begin{pmatrix} q \\ p \end{pmatrix} \mapsto \begin{pmatrix} A_{11} & A_{12} \\ A_{21} & A_{22} \end{pmatrix} \begin{pmatrix} q \\ p \end{pmatrix} + \frac{\kappa}{2\pi} \cos(2\pi q) \begin{pmatrix} A_{12} \\ A_{22} \end{pmatrix} \pmod{1}. \quad (3.1)$$

where $(q, p) \in \mathbb{T}^2$, $\mathbf{A} = \begin{pmatrix} A_{11} & A_{12} \\ A_{21} & A_{22} \end{pmatrix}$ is an $\text{SL}(2, \mathbb{Z})$ matrix, and κ is a small perturbation. The notation (q, p) is meant to evoke position and conjugate momentum forming a toral phase space, which is the identification made for quantization. Demanding wavefunctions respect the periodicity of the torus (set to unity²) in both q and its Fourier partner p yields a finite dimensional Hilbert space with rational Planck's constant $h = 1/N$ where N is the Hilbert space dimension [41, 42]. The Hilbert space is spanned by position eigenstates $|q_j\rangle$ delta-localized to $q_j = j/N$ for $j = 0, \dots, N-1$ (more generally, the index is identified modulo N). For a given classical map defined by \mathbf{A} and κ , the quantized unitary map U is computed by taking the semiclassical propagator to be exact [41, 43].³

The quantum cat map at a given dimension N has several number-theoretic symmetries [24, 44, 45]. We will focus in particular on the symmetries examined by Esposti and Winn [24]:⁴

1. **Abelian symmetry.** These include the momentum shift R and inversion W . R occurs when the dimension N is an integer multiple of $s := \text{gcd}(A_{12}, A_{22} - 1)$ for odd A_{12} , where gcd is the greatest common divisor. Then the momentum kick

$$R|q_j\rangle = \exp\left(i\frac{2\pi j}{s}\right)|q_j\rangle \quad (3.2)$$

commutes with the dynamics U and generates a symmetry group \mathbb{Z}_s . W is the quantization of the classical map

$$\begin{pmatrix} q \\ p \end{pmatrix} \mapsto \begin{pmatrix} \frac{1}{2} - q \\ \frac{1}{2} - p \end{pmatrix} \quad (3.3)$$

²Setting the periodicity of torus to unity can be thought of as a rescaling of units.

³The general expression for U is too involved to explain in the main text. See Appx. A for details.

⁴The symmetries discussed in Esposti and Winn [24] are symmetries of the unperturbed ($\kappa = 0$) quantum cat map. For some particular choices of perturbations, such as the map (3.1), they are symmetries of the perturbed ($\kappa > 0$) quantum cat map as well.

which takes the form

$$W |q_j\rangle = (-1)^j |q_{\frac{N}{2}-j}\rangle \quad (3.4)$$

for even dimension N . The W operator commutes with the dynamics U when N is divisible by 4 and generates a \mathbb{Z}_2 symmetry.

2. **Anticommuting unitary.** When N is even but *not* divisible by 4, and with particular constraints on \mathbf{A} , the W operator anticommutes with U . This is proved in Appx. A.3. The existence of an anticommuting unitary induces a pseudospin structure in the unitary dynamics:

$$U = \sigma_z \otimes \bar{U} \quad (3.5)$$

where σ_z is the Pauli-z matrix acting on a pseudospin, and \bar{U} a unitary. The details of this are discussed in Sect. 5.2.

3. **Non-Abelian symmetries.** The R and W operators do not commute, and so generate a non-Abelian symmetry algebra when both symmetries are present. The irreducible representations of the algebra must be either one-dimensional (simultaneous eigenspaces of R and W) or two-dimensional, since W exchanges two eigenvectors of R . Degeneracy of the representations when embedded in the cat map Hilbert space means each representation is tensored with a vector space on which the algebra acts trivially (as a multiple of identity). Representing such algebras is discussed in more detail in Sect. 6, while computation of the algebra generated by R and W is reserved for Appx. A.4.

In general, the energy spectra of the perturbed quantum cat maps possess random matrix statistics [43, 45, 46]. However, once R or W symmetry is present the spectral statistics deviate from random matrices, which can be interpreted as the superposition of spectra from independent symmetry sectors [24]. In the case of $\{W, U\} = 0$, equation (3.5) implies the quasi-energies appear in pairs $(E, E + \pi)$. Consequently only half of the quasi-energies show meaningful spectral statistics. The perturbed cat maps also display chaotic behavior, including Lyapunov growth and Ruelle-Pollicott resonance, for various other measures of chaos such as out-of-time-ordered correlators (OTOC) [25–28, 47–49].

3.2 Cumulative AFL in Quantum Cat Map

For simplicity, we fix the perturbation strength to be $\kappa = 0.05$ throughout our calculations. We compute the cumulative AFL entropy with respect to the maximally mixed state and choose the partitions to always be commuting projectors (that is, $[X^i, X^j] = 0$ and $(X^i)^2 = X^i = X^{i\dagger}$). Cumulative AFL is nondecreasing under such a partition, as the resulting channel $\mathcal{E}_\chi \otimes \mathbb{1}$ on the system and purifier is doubly stochastic [50].⁵ Generally, the cumulative AFL entropy gets exponentially close to the dimensional bound (2.11) at late times [12, 16].

⁵Doubly stochastic channels are completely positive, trace preserving, and unital (sends $\mathbb{1} \mapsto \mathbb{1}$). This means that $\mathbb{1} = \sum_i X^{i\dagger} X^i = \sum_i X^i X^{i\dagger}$. Such channels do not decrease von Neumann entropy [50].

For partitions that do not respect any symmetry, we choose to have $\mathcal{O}(1)$ -many projectors that are diagonal in a random basis, which we call a **random partition**. For chaotic dynamics, under such a partition the cumulative AFL entropy is expected to asymptote to the dimensional bound $S(\rho) + \log N = 2 \log N$. For partitions respecting an abelian symmetry Λ , we choose a random partition independently in each charge sector, which we call a **Λ -symmetric partition**. For partitions respecting an anticommuting unitary, we pick a **tensor product partition** which is the product of a channel on the pseudospin space (e.g. pseudospin-z measurement or identity channel) and a random partition on the non-pseudospin space. For partitions respecting a non-Abelian symmetry, we notice that a Λ -symmetric partition is built from partitions in the trivial space of each one-dimensional irrep of the Abelian symmetry. Generalizing this, we construct a **commutant partition** by, for each irrep of the algebra, choosing a random partition in the corresponding space the algebra acts trivially on. This implies each Kraus operator commutes with the whole algebra (in other words, they are in the commutant). See Sect. 4, 5, 6 for more general conditions and full explanations of the numerics. Our code is available on Github at [51].

1. **Abelian symmetries.** For the R operator, we choose the classical cat map matrix

$$\mathbf{A} = \begin{pmatrix} 6 & 5 \\ 7 & 6 \end{pmatrix} \quad (3.6)$$

with $s = \gcd(A_{12}, A_{22} - 1) = 5$. If $N = sM$, the dynamics decomposes into s charge sectors of dimension M . The cumulative AFL entropy is shown in Fig. 3a. When the dynamics and partition are both R -symmetric, the late-time saturation of H_{AFL} reduces from $2 \log N$ to $2 \log M + \log s$, as one might expect of independent/uncoupled dynamics. We may interpret the $\log s$ as the Shannon entropy of choosing which sector to start in.

For the W operator, we choose the classical cat map matrix

$$\mathbf{A} = \begin{pmatrix} 2 & 1 \\ 3 & 2 \end{pmatrix} \quad (3.7)$$

which has no nontrivial R symmetry, but commutes with W when $4|N$. The cumulative AFL for this case is plotted in Fig. 3b. The W operator has two charge sectors, and correspondingly H_{AFL} saturates to $2 \log(N/2) + \log 2$ when the partition is W -symmetric, instead of the usual $2 \log N$.

2. **Anticommuting unitary operator.** When N is even but not divisible by 4, the dynamics U of the map (3.7) obeys the anticommutation condition $\{W, U\} = 0$. In Fig. 4, we compare random partitions on the whole space to tensor product partitions with pseudospin-z measurement and no pseudospin measurement (identity channel). The respective bounds are $2 \log N$, $2 \log(N/2) + \log 2$, and $2 \log(N/2)$ as shown. The pseudospin dynamics are σ_z , which contributes a constant one bit ($\log 2$) of entropy when measured.

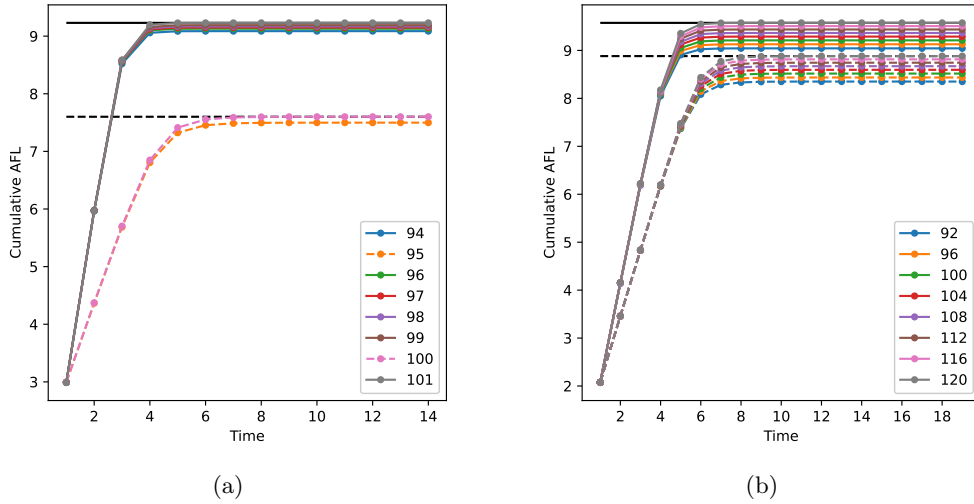


Figure 3: Abelian symmetries. Figure (a) shows the cumulative AFL entropy of the cat map $\mathbf{A} = \begin{pmatrix} 6 & 5 \\ 7 & 6 \end{pmatrix}$ with an R -symmetric partition for varying dimensions listed in the legend. R is a symmetry for dimensions 95 and 100 (dashed lines) only. The horizontal black lines show bounds for the largest dimensions plotted: $2 \log N$ in the nonsymmetric case with $N = 101$ (solid black), and $2 \log(N/5) + \log 5$ in the case with R -symmetry and $N = 100$ (dashed black). Figure (b) shows the cumulative AFL entropy of $\mathbf{A} = \begin{pmatrix} 2 & 1 \\ 3 & 2 \end{pmatrix}$ with random partitions (solid lines) compared to W -symmetric partitions (dashed lines). The horizontal black lines show the bounds for the largest dimension plotted ($N = 120$): $2 \log N$ in the random-partition case (solid black), and $2 \log(N/2) + \log 2$ in the W -symmetric partition case (dashed black).

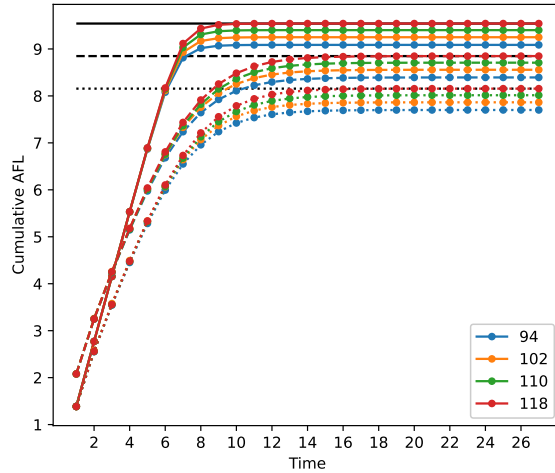


Figure 4: Anticommuting unitary. Plotted is the cumulative AFL entropy of the cat map for $\mathbf{A} = \begin{pmatrix} 2 & 1 \\ 3 & 2 \end{pmatrix}$. The figure compares random partitions (solid lines), measuring pseudospin-z (dashed lines), and no pseudospin measurement (dotted lines). The respective bounds of $2 \log N$, $2 \log(N/2) + \log 2$, and $2 \log(N/2)$ for $N = 118$ are shown by the horizontal black lines.

3. Non-Abelian symmetry. We choose the cat map matrix (3.6) and Hilbert space dimension $N = 100$ (divisible by 4 and by $s = 5$) so that both the R and W sym-

metries are present. The cumulative AFL entropy is plotted in Fig. 5 for random, symmetric, and commutant partitions. The random, R -symmetric, and W -symmetric have respective bounds of $2 \log N$, $2 \log M + \log s$, and $2 \log(N/2) + \log 2$ as discussed previously, but the commutant partition is even lower. The precise form of the bound is explained in Sect. 6.

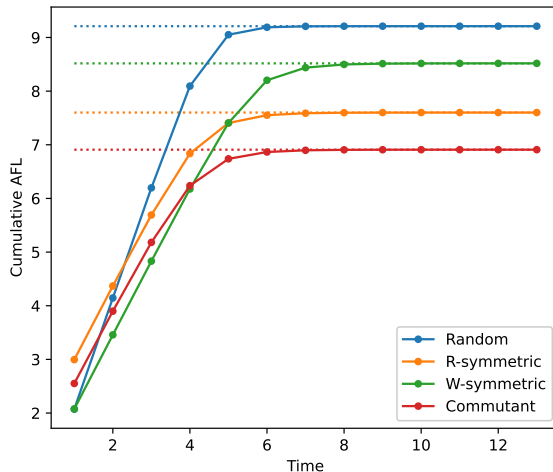


Figure 5: Non-Abelian symmetry. Plotted is the cumulative AFL entropy of the $\mathbf{A} = \begin{pmatrix} 6 & 5 \\ 7 & 6 \end{pmatrix}$ quantum cat map with dimension $N = 100$. The figure compares a random partition, R and W symmetric partitions, and a commutant partition. The dashed horizontal lines show the expected bounds in each case.

4 Abelian Symmetry

Below we provide rigorous results on H_{AFL} in the presence of Abelian symmetries and apply them to explain the results depicted in Fig 3. To clean up notation, we drop the S subscript from the system Hilbert space ($\mathcal{H} = \mathcal{H}_S$).

Take a Hermitian operator Z on a finite-dimensional Hilbert space \mathcal{H} (in our numerics, we have $Z = W$ or $Z = R$, and \mathcal{H} is the system Hilbert space \mathcal{H}_S). We may diagonalize the operator as $Z = \sum_{\lambda, \ell} z_{\lambda} |\lambda, \ell\rangle\langle\lambda, \ell|$ where $\lambda = 1, \dots, d$ index the distinct eigenvalues z_{λ} of Z , and ℓ runs over the degeneracy. Any such eigenbasis of Z decomposes the Hilbert space into orthogonal subspaces $\mathcal{H}_{\lambda} = \text{span}\{|\lambda, \ell\rangle\}_{\ell}$ such that $\mathcal{H} = \bigoplus_{\lambda} \mathcal{H}_{\lambda}$. We will also refer to \mathcal{H}_{λ} as a charge sector. Now consider some linear operator Q on \mathcal{H} that commutes with Z . Since Z acts as a multiple of identity on \mathcal{H}_{λ} , $[Q, Z] = 0$ if and only if Q is block diagonal in any eigenbasis of Z with vectors grouped by charge. In such a basis, the matrices of Z and Q take the form

$$Z = \begin{pmatrix} \boxed{z_1 \mathbf{1}} & & \mathbf{0} \\ & \ddots & \\ \mathbf{0} & & \boxed{z_d \mathbf{1}} \end{pmatrix} \text{ and } Q = \begin{pmatrix} \boxed{Q_1} & & \mathbf{0} \\ & \ddots & \\ \mathbf{0} & & \boxed{Q_d} \end{pmatrix} \quad (4.1)$$

where $Q_\lambda = Q|_{\mathcal{H}_\lambda}$ is the restriction of Q to the λ^{th} charge sector and $Q = \bigoplus_\lambda Q_\lambda$. We will occasionally abuse notation and also use Q_λ to refer to the projection $\sum_\ell \langle \lambda, \ell | Q | \lambda, \ell \rangle | \lambda, \ell \rangle \langle \lambda, \ell |$ acting on full Hilbert space \mathcal{H} . We will note a few final aspects and notations of operators commuting with Z :

1. Due to the block diagonal structure, there are no cross terms when composing direct-sum operators. Given any two operators, Q and Q' , that both commute with Z , we have

$$QQ' = \left(\bigoplus_\lambda Q_\lambda \right) \left(\bigoplus_\lambda Q'_\lambda \right) = \bigoplus_\lambda Q_\lambda Q'_\lambda \quad (4.2)$$

or pictorially

$$\begin{pmatrix} \boxed{Q_1} & & \mathbf{0} \\ & \ddots & \\ \mathbf{0} & & \boxed{Q_d} \end{pmatrix} \begin{pmatrix} \boxed{Q'_1} & & \mathbf{0} \\ & \ddots & \\ \mathbf{0} & & \boxed{Q'_d} \end{pmatrix} = \begin{pmatrix} \boxed{Q_1 Q'_1} & & \mathbf{0} \\ & \ddots & \\ \mathbf{0} & & \boxed{Q_d Q'_d} \end{pmatrix}$$

2. If the operator commuting with Z is a density matrix ρ , we will alter the notation by rescaling the restriction in the following way:

$$\rho = \bigoplus_\lambda p_\lambda \rho_\lambda, \quad \text{for } p_\lambda = \text{Tr}(\rho|_{\mathcal{H}_\lambda}) \text{ and } \rho_\lambda = \frac{1}{p_\lambda} \rho|_{\mathcal{H}_\lambda}. \quad (4.3)$$

Note with this convention, ρ_λ is a density matrix on \mathcal{H}_λ and $\{p_\lambda\}$ is a probability distribution.

3. Given a partition of unity $\mathcal{X} = \{X^1, \dots, X^K\}$ on \mathcal{H} , if all the operators in \mathcal{X} commute with Z then the set of restrictions to \mathcal{H}_λ is a partition of unity on \mathcal{H}_λ , which we denote $\mathcal{X}_\lambda = \{X_\lambda^1, \dots, X_\lambda^K\}$. As matrices, this looks like

$$\sum_i \begin{pmatrix} \boxed{X_1^{i\dagger}} & & \mathbf{0} \\ & \ddots & \\ \mathbf{0} & & \boxed{X_d^{i\dagger}} \end{pmatrix} \begin{pmatrix} \boxed{X_1^i} & & \mathbf{0} \\ & \ddots & \\ \mathbf{0} & & \boxed{X_d^i} \end{pmatrix} = \begin{pmatrix} \boxed{\mathbf{1}_{\mathcal{H}_1}} & & \mathbf{0} \\ & \ddots & \\ \mathbf{0} & & \boxed{\mathbf{1}_{\mathcal{H}_d}} \end{pmatrix} \quad (4.4)$$

4.1 Theorem 1

For convenience, we denote the Shannon entropy of a probability distribution $\{p_i\}$ as $H_S(\{p_i\}) = -\sum_i p_i \log p_i$. We have the following theorem regarding H_{AFL} in the presence of a symmetry operator Z :

Theorem 1. *If the dynamics U , density matrix ρ , and all the operators in the partition \mathcal{X} commute with a Hermitian operator Z , then*

$$H_{\text{AFL}}(\rho, U, \mathcal{X}, t) \leq \sum_\lambda p_\lambda H_{\text{AFL}}(\rho_\lambda, U_\lambda, \mathcal{X}_\lambda, t) + H_S(\{p_\lambda\}) \quad (4.5)$$

with equality if the measurement channel admits a Kraus representation where $X^i \in \mathcal{X}$ have support on exactly one charge sector each.

The equality condition means there is a map ϕ from a Kraus index to the corresponding charge index. We can then write

$$X_\lambda^i = X^i|_{\mathcal{H}_\lambda} = \delta(\phi(i) = \lambda)X_{\phi(i)}^i \quad (4.6)$$

or visually as

$$X^i = \begin{pmatrix} \boxed{X_1^i} & & \mathbf{0} \\ & \ddots & \\ \mathbf{0} & & \boxed{X_d^i} \end{pmatrix} = \begin{pmatrix} \boxed{\mathbf{0}} & & & \mathbf{0} \\ & \ddots & & \\ & & \boxed{X_{\phi(i)}^i} & \\ \mathbf{0} & & & \boxed{\mathbf{0}} \end{pmatrix}$$

Intuitively, the full dynamics is a set of independent dynamics on each charge sector. If our measurements and state respect this, then the resulting dynamics in the environment are also independent and combine with weights $\{p_\lambda\}$ to form the full distribution. Thus, their entropies add (weighted by the state) with an additional Shannon entropy corresponding to the uncertainty of picking which sector to start in.

The cumulative AFL entropy on a maximally mixed state with an R - or W -symmetric partition, as we plot in Fig. 3, falls under Thm. 1. The dynamics splits into s charge sectors of dimension M and the state is maximally mixed, so the distribution p_λ is a uniform $1/s$. This means $H_S(\{p_\lambda\}) = \log s$ and the dimensional upper bound (2.11) in each sector is $2 \log M$. Thus, the cumulative AFL entropy at all times is bounded above by

$$H_{\text{AFL}} \leq 2 \log M + \log s, \quad (4.7)$$

as we observe in our numerics.

4.2 Proof of Theorem 1

Proof. We will prove Theorem 1 in the environment Hilbert space. Another proof using states in the system and purifier spaces can be found in Appx. B. Before proceeding, recall that von Neumann entropy obeys the following inequality for a convex sum $\rho = \sum_i p_i \rho_i$,

$$S(\rho) \leq \sum_i p_i S(\rho_i) + H_S(\{p_i\}) \quad (4.8)$$

with equality if the set of ρ_i have orthogonal support [31].

After t time steps, the multitime Kraus operators of the measurement channel are indexed by $\mathbf{i} = (i_1, \dots, i_t)$. The kets $|\mathbf{i}\rangle$ are a basis of the environment Hilbert space, as in

equation (2.1). The state of the measurement device is

$$\begin{aligned}
\tilde{\rho}[(U\mathcal{X})^t]_{ij} &= \langle \mathbf{i} | \tilde{\rho}[(U\mathcal{X})^t] | \mathbf{j} \rangle \\
&= \text{Tr} \left(UX^{i_t} \dots UX^{i_1} \rho X^{j_1 \dagger} U^\dagger \dots X^{j_t \dagger} U^\dagger \right) \\
&= \sum_{\lambda} p_{\lambda} \text{Tr} \left(U_{\lambda} X_{\lambda}^{i_t} \dots U_{\lambda} X_{\lambda}^{i_1} \rho_{\lambda} X_{\lambda}^{j_1 \dagger} U_{\lambda}^{\dagger} \dots X_{\lambda}^{j_t \dagger} U_{\lambda}^{\dagger} \right) \\
&= \sum_{\lambda} p_{\lambda} \tilde{\rho}_{\lambda}[(U_{\lambda} \mathcal{X}_{\lambda})^t]_{ij}
\end{aligned} \tag{4.9}$$

where we have used the fact that U, ρ , and \mathcal{X} all admit a block diagonal structure due to their commutation relation with Z , and $\tilde{\rho}_{\lambda}[(U_{\lambda} \mathcal{X}_{\lambda})^t]$ is the state of the measurement device if the system had started in ρ_{λ} .⁶ It follows from (4.8) that

$$S(\tilde{\rho}[(U\mathcal{X})^t]) \leq \sum_{\lambda} p_{\lambda} S(\tilde{\rho}_{\lambda}[(U_{\lambda} \mathcal{X}_{\lambda})^t]) + H_S(\{p_{\lambda}\}). \tag{4.10}$$

Next, we prove the equality is achieved when the measurement channel admits a Kraus representation where $X^i \in \mathcal{X}$ have support on exactly one charge sector each. In general, while the set of ρ_{λ} have orthogonal support, the same is not necessarily true of $\tilde{\rho}_{\lambda}$, preventing equality. However, if each Kraus operator in \mathcal{X} has support on exactly one charge sector, we will show that the $\tilde{\rho}_{\lambda}$ do indeed have orthogonal support.

It follows from equation (4.6) that $X_{\lambda}^i U_{\lambda} X_{\lambda}^j$ is nonzero only if $\phi(i) = \phi(j) = \lambda$. Thus, we have

$$\tilde{\rho}_{\lambda}[(U_{\lambda} \mathcal{X}_{\lambda})^t]_{ij} \propto \delta(\mathbf{i} \sim \lambda) \delta(\mathbf{j} \sim \lambda) \tag{4.11}$$

where $\mathbf{i} \sim \lambda$ is shorthand for $\phi(i_k) = \lambda$ for all $k = 1, \dots, t$. This means the support of $\tilde{\rho}_{\lambda}$ is a subspace of $\text{span}\{|\mathbf{j}\rangle \in \mathcal{H}_E \mid \mathbf{j} \sim \lambda\}$, which can be explicitly seen from the relation

$$\tilde{\rho}_{\lambda} |\mathbf{j}\rangle = \sum_{\mathbf{i}} [\tilde{\rho}_{\lambda}]_{ij} |\mathbf{i}\rangle \propto \delta(\mathbf{j} \sim \lambda) \tag{4.12}$$

Consider now $\tilde{\rho}_{\mu}$ with $\mu \neq \lambda$, whose support is a subspace of $\text{span}\{|\mathbf{j}\rangle \in \mathcal{H}_E \mid \mathbf{j} \sim \mu\}$. Given a fixed vector $|\mathbf{j}\rangle$, since each index j_k belongs to only one charge sector $\phi(j_k)$, one cannot have both $\mathbf{j} \sim \mu$ and $\mathbf{j} \sim \lambda$. In other words, $|\mathbf{j}\rangle$ cannot be in both supports. Thus, the supports are orthogonal as desired. \square

5 Tensor Product Dynamics

Having studied dynamics with a direct sum structure, we now turn to dynamics with a tensor product structure. We will see in Section 5.2 that the anticommuting unitary is a special case. Let the Hilbert space be a tensor product $\mathcal{H} = \mathcal{H}_A \otimes \mathcal{H}_B$ and ρ be a separable state, meaning there is a decomposition

$$\rho = \sum_{\nu} q^{\nu} \rho_A^{\nu} \otimes \rho_B^{\nu} \tag{5.1}$$

⁶We mean the initial state of the system was $\mathbf{0} \oplus \rho_{\lambda} \oplus \mathbf{0}$ where the zeros cover all charge with index differing from λ .

where ρ_A^ν, ρ_B^ν are states on $\mathcal{H}_A, \mathcal{H}_B$ respectively, and $\{q^\nu\}$ is a probability distribution. We will consider dynamics and measurements that act “locally” on subsystems A and B . Explicitly, $U = U_A \otimes U_B$, and given partitions \mathcal{X}_A and \mathcal{X}_B on \mathcal{H}_A and \mathcal{H}_B respectively, the measurement channel takes the form

$$\mathcal{X} = \mathcal{X}_A \otimes \mathcal{X}_B = \{ X_A \otimes X_B \mid X_A \in \mathcal{X}_A, X_B \in \mathcal{X}_B \} \quad (5.2)$$

This partition corresponds to measuring the subsystems independently.

5.1 Theorem 2

Theorem 2. *With the separable state $\rho = \sum_\nu q^\nu \rho_A^\nu \otimes \rho_B^\nu$, tensor product dynamics $U = U_A \otimes U_B$, and partition $\mathcal{X} = \mathcal{X}_A \otimes \mathcal{X}_B$ given above, the cumulative AFL entropy obeys*

$$H_{\text{AFL}}(\rho, U, \mathcal{X}, t) \leq \sum_\nu q^\nu [H_{\text{AFL}}(\rho_A^\nu, U_A, \mathcal{X}_A, t) + H_{\text{AFL}}(\rho_B^\nu, U_B, \mathcal{X}_B, t)] + H_S(\{q^\nu\}) \quad (5.3)$$

The generalization to multipartite systems is obvious. In some special cases, we get simpler equalities:

1. If the partition \mathcal{X}_B is a unitary channel (a single unitary Kraus operator, typically $\mathbb{1}_B$), then we have

$$H_{\text{AFL}}(\rho, U, \mathcal{X}, t) = H_{\text{AFL}}(\rho_A, U_A, \mathcal{X}_A, t) \quad (5.4)$$

where $\rho_A = \sum_\nu q^\nu \rho_A^\nu = \text{Tr}_B(\rho)$ is the reduced state of system A . Intuitively, we are not measuring system B and so the dynamical entropy reduces to that of A .

2. If ρ is a product state $\rho_A \otimes \rho_B$, then

$$H_{\text{AFL}}(\rho, U, \mathcal{X}, t) = H_{\text{AFL}}(\rho_A, U_A, \mathcal{X}_A, t) + H_{\text{AFL}}(\rho_B, U_B, \mathcal{X}_B, t) \quad (5.5)$$

as we would expect of independent dynamics.

5.2 Anticommuting Unitary

One way to guarantee tensor product dynamics is the existence of an anticommuting unitary. Consider a unitary W that anticommutes with the dynamics U (we use the notation W deliberately, as this is the form of the anticommuting unitary in the cat map example discussed in Sect. 3). Given $U|\phi\rangle = e^{i\phi}|\phi\rangle$ for $\phi \in [0, 2\pi)$, then $W|\phi\rangle$ is also an eigenstate of U with eigenvalue $-e^{i\phi} = e^{i(\phi+\pi)}$. Since $-e^{i\phi} \neq e^{i\phi}$ for all ϕ , the Hilbert space must be even dimensional and splits into two spaces of equal dimension: $\mathcal{H} = \overline{\mathcal{H}} \oplus W\overline{\mathcal{H}}$ with $\overline{\mathcal{H}}$ the eigenspace for phases $\phi \in [0, \pi)$. We can identify these two spaces as a pseudospin-1/2 degree of freedom and write $\mathcal{H} \cong \mathbb{C}^2 \otimes \overline{\mathcal{H}}$, where \mathbb{C}^2 notates a 2-dimensional complex vector

space. In some basis respecting the pseudospin, we have

$$U = \sigma_z \otimes \bar{U} \quad \text{and} \quad W = \sigma_x \otimes \bar{W} \quad (5.6)$$

or as matrices

$$U = \begin{pmatrix} \boxed{\bar{U}} & \mathbf{0} \\ \mathbf{0} & \boxed{-\bar{U}} \end{pmatrix} \quad \text{and} \quad W = \begin{pmatrix} \mathbf{0} & \boxed{\bar{W}} \\ \boxed{\bar{W}} & \mathbf{0} \end{pmatrix}$$

where $\bar{U} = U|_{\bar{\mathcal{H}}}$ and \bar{W} is a unitary on $\bar{\mathcal{H}}$ commuting with \bar{U} .

The induced tensor product structure allows us to make use of Thm. 2 in the presence of an anticommuting unitary, such as for the cat map in Fig. 4. There, we consider two tensor product partitions, one measuring pseudospin-z and one with no pseudospin measurement. Explicitly, the partitions on the \mathbb{C}^2 pseudospin space are $\mathcal{X}_{\mathbb{C}^2} = \{|\uparrow\rangle\langle\uparrow|, |\downarrow\rangle\langle\downarrow|\}$ and $\mathcal{X}_{\mathbb{C}^2} = \{\mathbb{1}_2\}$ respectively. The pseudospin-z measurement falls under the special case (5.5), as the maximally mixed state is a product state

$$\rho = \frac{1}{N} \mathbb{1}_N = \frac{1}{2} \mathbb{1}_2 \otimes \frac{1}{N/2} \mathbb{1}_{N/2}. \quad (5.7)$$

The cumulative AFL entropy on $\bar{\mathcal{H}}$ is dimensionally bounded by $2 \log \dim \bar{\mathcal{H}} = 2 \log(N/2)$. The pseudospin space adds a constant entropy of $\log 2$ at all times. This is because the pseudospin dynamics are σ_z , so the pseudospin-z measurement simply contributes one bit of information: which pseudospin-z sector the state begins in. Thus, the dimensional bound of H_{AFL} has lowered from $2 \log N$ to

$$H_{\text{AFL}} \leq 2 \log(N/2) + \log 2. \quad (5.8)$$

The case of no pseudospin measurement falls under (5.4), so the $\log 2$ from the pseudospin space is absent, consistent with our numerics.

5.3 Proof of Theorem 2

Proof. The partition after t time steps is indexed by two vectors \mathbf{a}, \mathbf{b} with

$$(U\mathcal{X})_{\mathbf{ab}}^t = (U_A X_A^{a_t} \cdots U_A X_A^{a_1}) \otimes (U_B X_B^{b_t} \cdots U_B X_B^{b_1}) \quad (5.9)$$

Indexing the rows by vectors \mathbf{ab} and columns by $\alpha\beta$, the state of the environment is

$$\begin{aligned}
\tilde{\rho}[(U\mathcal{X})^t]_{\mathbf{ab};\alpha\beta} &= \sum_{\nu} q^{\nu} \text{Tr} \left((U_A X_A^{a_t} \cdots U_A X_A^{a_1}) \otimes (U_B X_B^{b_t} \cdots U_B X_B^{b_1}) \rho_A^{\nu} \otimes \rho_B^{\nu} \right. \\
&\quad \left. (U_A X_A^{\alpha_t} \cdots U_A X_A^{\alpha_1})^{\dagger} \otimes (U_B X_B^{\beta_t} \cdots U_B X_B^{\beta_1})^{\dagger} \right) \\
&= \sum_{\nu} q^{\nu} \text{Tr} \left(U_A X_A^{a_t} \cdots U_A X_A^{a_1} \rho_A^{\nu} X_A^{\alpha_1 \dagger} U_A^{\dagger} \cdots X_A^{\alpha_t \dagger} U_A^{\dagger} \right) \\
&\quad \times \text{Tr} \left(U_B X_B^{b_t} \cdots U_B X_B^{b_1} \rho_B^{\nu} X_B^{\beta_1 \dagger} U_B^{\dagger} \cdots X_B^{\beta_t \dagger} U_B^{\dagger} \right) \\
&= \sum_{\nu} q^{\nu} \tilde{\rho}_A^{\nu} [(U_A \mathcal{X}_A)^t]_{\mathbf{a}\alpha} \tilde{\rho}_B^{\nu} [(U_B \mathcal{X}_B)^t]_{\mathbf{b}\beta} \tag{5.10}
\end{aligned}$$

\Downarrow

$$\tilde{\rho}[(U\mathcal{X})^t] = \sum_{\nu} q^{\nu} \tilde{\rho}_A^{\nu} [(U_A \mathcal{X}_A)^t] \otimes \tilde{\rho}_B^{\nu} [(U_B \mathcal{X}_B)^t] \tag{5.11}$$

Since the von Neumann entropy of a product state is additive, $S(\rho \otimes \sigma) = S(\rho) + S(\sigma)$, applying the convex sum inequality (4.8) gives the desired result.

Now we turn to the special cases. If \mathcal{X}_B is a unitary channel, then $(U_B \mathcal{X}_B)^t$ is also a unitary channel with only one Kraus operator. Thus, $\tilde{\rho}_B^{\nu}$ is simply the scalar 1 and can be dropped from (5.11). By linearity of the trace,

$$\sum_{\nu} q^{\nu} \tilde{\rho}_A^{\nu} = \tilde{\rho}_A \tag{5.12}$$

for $\rho_A = \sum_{\nu} q^{\nu} \rho_A^{\nu}$ the reduced state on A , which gives us case (5.4).

Now making no assumptions of \mathcal{X}_B but restricting the state ρ to be a product state $\rho_A \otimes \rho_B$, the sum over ν is absent. With no need to use the inequality (4.8), the proof above immediately yields the equality (5.5). \square

6 Non-Abelian Symmetries

The direct sum and tensor product structures naturally combine when we generalize from a single symmetry operator Z to a (von Neumann) algebra of symmetry operators \mathcal{A} on \mathcal{H} all commuting with U . For simplicity, we assume $\mathbf{1}_{\mathcal{H}} \in \mathcal{A}$. Let \mathcal{Z} be the center of \mathcal{A} and $d = \dim \mathcal{Z}$. Since \mathcal{Z} is Abelian, it has a diagonal representation $\mathcal{Z} = \bigoplus_{\lambda} \mathbb{C} \mathbf{1}_{\mathcal{H}_{\lambda}}$ on $\mathcal{H} = \bigoplus_{\lambda} \mathcal{H}_{\lambda}$, where $\lambda = 1, \dots, d$ label the (one-dimensional) irreps of the center [52]. Each subspace \mathcal{H}_{λ} can be further decomposed as a tensor product of two spaces, one from \mathcal{A} acting irreducibly on (call it \mathcal{K}_{λ}), the other from \mathcal{A} acting trivially on (call it \mathcal{K}'_{λ}). Thus, we have an overall decomposition

$$\mathcal{H} = \bigoplus_{\lambda=1}^d \mathcal{K}_{\lambda} \otimes \mathcal{K}'_{\lambda}. \tag{6.1}$$

We will set $\dim \mathcal{K}_{\lambda} = n_{\lambda}$ and $\dim \mathcal{K}'_{\lambda} = n'_{\lambda}$. With this decomposition, the symmetry algebra takes the form

$$\mathcal{A} \cong \bigoplus_{\lambda=1}^d \mathcal{L}(\mathcal{H}_{\lambda}) \otimes \mathbf{1}_{n'_{\lambda}} \tag{6.2}$$

where $\mathcal{L}(\mathcal{H}_\lambda)$ is all linear operators on \mathcal{H}_λ . Since the dynamics U commutes with the entire algebra \mathcal{A} , it must be of the form

$$U = \bigoplus_{\lambda=1}^d \mathbb{1}_{n_\lambda} \otimes U_\lambda \quad (6.3)$$

where U_λ is the restriction $U|_{\mathcal{K}'_\lambda}$. Visually, in a basis respecting the decomposition (6.1), the dynamics has the matrix representation

$$U = \begin{pmatrix} \boxed{\lambda=1} & & \mathbf{0} \\ & \ddots & \\ \mathbf{0} & & \boxed{\lambda=d} \end{pmatrix} \quad \text{with} \quad \boxed{\lambda} = \begin{pmatrix} \boxed{U_\lambda} & & \mathbf{0} \\ & \ddots & \\ \mathbf{0} & & \boxed{U_\lambda} \end{pmatrix} \quad (6.4)$$

For further discussion and examples of this structure, see [52–55].

For clarity, we can explicitly show this formalism subsumes the previous case of a single symmetry operator Z . Consider the case where \mathcal{A} is Abelian. Then $\mathcal{A} = \mathcal{Z} = \bigoplus_\lambda \mathbb{C} \mathbb{1}_{\mathcal{H}_\lambda}$, which induces the same decomposition as a single symmetry operator $Z = \bigoplus_\lambda z_\lambda \mathbb{1}_{\mathcal{H}_\lambda}$ for some set of distinct scalars $\{z_\lambda\}$. This construction also goes the other way, as Z generates \mathcal{A} .

Now we return to the H_{AFL} inequalities. Given a symmetry algebra \mathcal{A} commuting with the dynamics, then U takes the form (6.3) which is a direct sum over tensor product dynamics. The obvious extension of our prior requirements is for the state to commute with the center \mathcal{Z} and be separable in each charge sector:

$$\rho = \bigoplus_{\lambda} \sum_{\nu} p_{\lambda}^{\nu} \rho_{\lambda}^{\nu} \otimes \rho_{\lambda}^{\nu} \quad (6.5)$$

where $\{p_{\lambda}^{\nu}\}$ is a probability distribution over (λ, ν) and $\rho_{\lambda}^{\nu}, \rho_{\lambda}^{\nu}$ density matrices on $\mathcal{K}_\lambda, \mathcal{K}'_\lambda$ respectively. Similarly, we require the partition to admit a form

$$\begin{aligned} \mathcal{X} &= \bigoplus_{\lambda} \mathcal{X}_\lambda \otimes \mathcal{X}'_\lambda \\ &= \left\{ \bigoplus_{\lambda} X_\lambda \otimes X'_\lambda \mid X_\lambda \in \mathcal{X}_\lambda, X'_\lambda \in \mathcal{X}'_\lambda, \right\} \end{aligned} \quad (6.6)$$

for partitions $\mathcal{X}_\lambda, \mathcal{X}'_\lambda$ on $\mathcal{K}_\lambda, \mathcal{K}'_\lambda$ respectively.

Theorem 3. *If the dynamics U commute with a von Neumann algebra \mathcal{A} , the state takes the form $\rho = \bigoplus_{\lambda} \sum_{\nu} p_{\lambda}^{\nu} \rho_{\lambda}^{\nu} \otimes \rho_{\lambda}^{\nu}$ and the partition admits a Kraus representation $\mathcal{X} = \bigoplus_{\lambda} \mathcal{X}_\lambda \otimes \mathcal{X}'_\lambda$ as defined above, then the cumulative AFL entropy obeys*

$$\begin{aligned} H_{\text{AFL}}(\rho, U, \mathcal{X}, t) &\leq \sum_{\lambda, \nu} p_{\lambda}^{\nu} [H_{\text{AFL}}(\rho_{\lambda}^{\nu}, \mathbb{1}_{n_\lambda}, \mathcal{X}_\lambda, t) \\ &\quad + H_{\text{AFL}}(\rho_{\lambda}^{\nu}, U_\lambda, \mathcal{X}'_\lambda, t)] + H_{\text{S}}(\{p_{\lambda}^{\nu}\}) \end{aligned} \quad (6.7)$$

If we choose \mathcal{X}_λ to be a partition of commuting Kraus operators (e.g. commuting projectors), then the cumulative AFL entropy on \mathcal{K}_λ (the first term) is a constant. If \mathcal{X}_λ is a unitary channel, then the term vanishes.

The commutant partition used for computing H_{AFL} in Fig. 5 falls under Thm. 3. Namely, we have $\mathcal{X}_\lambda = \{\mathbb{1}_{n_\lambda}\}$, \mathcal{X}'_λ a random partition, and a state

$$\rho = \frac{1}{N} \mathbb{1}_N = \bigoplus_{\lambda=1}^d p_\lambda \frac{1}{n_\lambda} \mathbb{1}_{n_\lambda} \otimes \frac{1}{n'_\lambda} \mathbb{1}_{n'_\lambda} \quad (6.8)$$

for Hilbert space dimension N and probability distribution $p_\lambda = n_\lambda n'_\lambda / N$. Thus, Thm. 3 yields a dimensional upper bound of

$$H_{\text{AFL}} \leq 2 \sum_{\lambda=1}^d p_\lambda \log n'_\lambda + H_S(\{p_\lambda\}). \quad (6.9)$$

For the algebra generated by the cat map symmetries R and W , as computed in Appx. A.4, the center has dimension $d = (s + 3)/2$. The dimensions of the irreps of the algebra are $n_1 = n_2 = 1$, and $n_\lambda = 2$ otherwise. The dimensions of the trivial spaces are $n'_1 = \frac{M}{2} + 1$, $n'_2 = \frac{M}{2} - 1$, and $n'_\lambda = M$ otherwise. Given these values, the bound (6.9) is computed and shown in Fig. 5. The cumulative AFL entropy under a commutant partition asymptotes to this bound as expected.

Proof. Theorem 3 follows immediately from Thm. 1 and 2, and the identity $H_S(\{p'_\lambda\}) = H_S(\{q_\lambda\}) + \sum_\lambda q_\lambda H_S(\{r_{\nu|\lambda}\})$ for marginal distribution $q_\lambda = \sum_\nu p'_\lambda$ and conditional distribution $r_{\nu|\lambda} = p'_{\lambda\nu} / q_\lambda$. Note p'_λ is a probability distribution over (λ, ν) but $r_{\nu|\lambda}$ is a distribution over ν only. \square

7 Discussions

The entropy rate h_{AFL} in (2.8), by definition, is partition-independent⁷, but in finite dimensions where cumulative AFL entropy is the appropriate quantity, the choice of partition plays an important role. Outside of comparing semiclassical partitions to random partitions [15], the effects of partition choice have—to our knowledge—not been studied. In this work, we showed how the presence of symmetries in the dynamics leads to dramatic dependence of H_{AFL} on partition choice. Specifically, the cumulative AFL entropy is insensitive to a given symmetry unless the measurements are chosen to respect the resulting symmetry structure in Hilbert space. Symmetries have important consequences for quantum chaos, and one rarely has full knowledge of the symmetries for a given dynamics. This means in practice that H_{AFL} may fail to fully diagnose the chaoticity of a given dynamics.

⁷There can still be some subtlety in infinite-dimensional systems over which space of partitions to take the supremum over [56].

7.1 Types of Quantum Chaos

Although the perturbed quantum cat map has random matrix spectral statistics, the unperturbed map does not [43, 45, 46]. Despite this, the map still has a semiclassically chaotic limit (see [57] for a review), in apparent violation of the Bohigas-Giannoni-Schmit (BGS) conjecture [17]. Indeed, the unperturbed cat map still displays Lyapunov growth in OTOC [25, 26] and H_{AFL} ,⁸ and obeys eigenstate thermalization [58]. However, as pointed out by Magan and Wu [59], spectral chaos (random matrix statistics) and basis/semiclassical chaos (eigenstate thermalization and Lyapunov growth) are actually distinct characteristics of quantum chaos, except when the Hamiltonian is k -local. The unperturbed cat map is an example of dynamics displaying only basis chaos. In this language, AFL entropy is a measure of basis chaos and exhibits limited sensitivity to spectral chaos. It is thus a diagnostic of semiclassical chaos and may not fully capture all aspects of *quantum* chaos.

7.2 Relation to CNT Entropy

The quantum dynamical entropies, as information theoretic quantities, are often related conceptually and can even bound one another using various quantum information constructions. Of particular importance, is the Holevo bound on the classical capacity of a quantum channel [31, 32]. Entropy exchange and AFL entropy upper bound instances of the Holevo quantity [13, 14, 33], and can be slightly modified to match it [60]. The other common quantum dynamical entropy construction by Stømer, Connes, Narnhofer, and Thirring (CNT) [2, 3] can be considered a generalization of the Holevo quantity to multiple channel inputs [61]. Some work has been done comparing CNT and AFL entropy more precisely [62–65]. These quantum dynamical entropies could play a crucial role in understanding quantum channel capacities and their relation with diagnostics of quantum chaos. We leave such explorations to future work.

Acknowledgments

The authors thank Nima Lashkari, Hong Liu, and Ayush Raj for inspiring discussions. K.F. acknowledges support from Prof. Ning Bao at Northeastern University.

A The Cat Map

A.1 Classical Cat Map

The classical cat map, first introduced by Arnol'd [40], is a map \mathbf{A} on the torus \mathbb{T}^2 with periodicity set to unit for convenience:

$$\mathbf{A} \begin{pmatrix} q \\ p \end{pmatrix} = \begin{pmatrix} A_{11} & A_{12} \\ A_{21} & A_{22} \end{pmatrix} \begin{pmatrix} q \\ p \end{pmatrix} \pmod{1}, \quad \text{for } \begin{pmatrix} q \\ p \end{pmatrix} \in \mathbb{T}^2. \quad (\text{A.1})$$

⁸Although not pictured, the behavior of H_{AFL} is nearly identical for the perturbed and unperturbed cat maps for partitions of projectors diagonal in the q -basis, p -basis, or a random basis, as well as various noncommutative combinations. It is reasonable to assume that fine-tuning the partition choice to the pseudosymmetries [44, 45] of the unperturbed map would distinguish these cases.

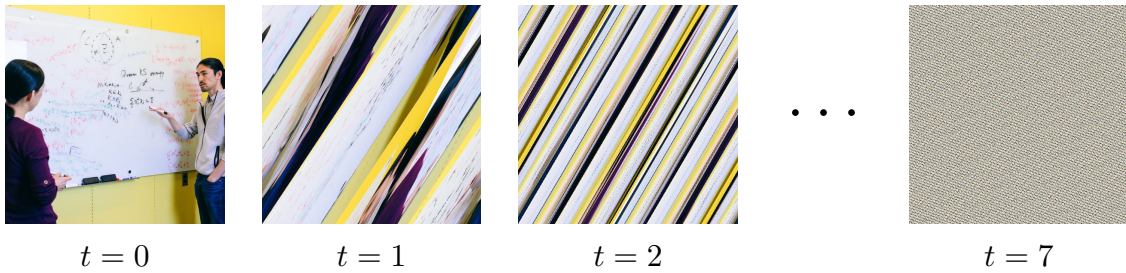


Figure 6: The action of the unperturbed classical cat map $\mathbf{A} = \begin{pmatrix} 2 & 1 \\ 3 & 2 \end{pmatrix}$ for t iterations.

With a slight abuse of notation, we will keep the modulo 1 implicit and use \mathbf{A} to refer to the matrix. Given $\mathbf{A} \in \text{SL}(2, \mathbb{Z})$ and $\text{Tr } \mathbf{A} > 2$, the cat map is continuous, area (Lebesgue measure) preserving, and hyperbolic. This makes the map chaotic (in fact, Anosov) with Lyapunov exponents given by $\log \lambda_+ > 0$ and $\log \lambda_- < 0$, where λ_{\pm} are the eigenvalues of \mathbf{A} . The KS entropy of the cat map is equal to the positive Lyapunov exponent $\log \lambda_+$ [40]. The action of an example classical cat map is shown in Fig. 6.

The cat map is structurally stable and can retain its chaotic (Anosov) properties in the presence of weak perturbations [40, 43, 66]. Specifically, the cat map is often studied with nonlinear shears in q or p , meaning the dynamical map takes the form $\mathbf{A} \circ \kappa_p G_p \circ \kappa_q F_q$, where

$$F_q \begin{pmatrix} q \\ p \end{pmatrix} = \begin{pmatrix} q + F(p) \\ p \end{pmatrix} \quad \text{and} \quad G_p \begin{pmatrix} q \\ p \end{pmatrix} = \begin{pmatrix} q \\ p + G(q) \end{pmatrix}. \quad (\text{A.2})$$

There is not a unique choice of shear, but the form of F and G is constrained by the periodicity of the torus and symmetries one wishes to retain or break, namely parity and time-reversal [45]. The case of no shears is referred to as the unperturbed cat map.

Our work uses a common choice of perturbation $G(q) = \frac{1}{2\pi} \cos(2\pi q)$, with $\kappa_q = 0$ and $\kappa_p := \kappa$. This shear is even in q , and so breaks parity but preserves time-reversal. The resulting cat map is

$$(\mathbf{A} \circ \kappa G_p) \begin{pmatrix} q \\ p \end{pmatrix} = \begin{pmatrix} A_{11} & A_{12} \\ A_{21} & A_{22} \end{pmatrix} \begin{pmatrix} q \\ p \end{pmatrix} + \frac{\kappa}{2\pi} \cos(2\pi q) \begin{pmatrix} A_{12} \\ A_{22} \end{pmatrix} \pmod{1}. \quad (\text{A.3})$$

A.2 Quantizing the Cat Map

The quantization of the unperturbed cat map was first derived by Hannay and Berry [41] based on earlier work on quantum maps [67]. Following work by Matos and Almeida [43] extended the derivation to the perturbed maps. The quantization follows by identifying $(q, p) \in \mathbb{T}^2$ as conjugate position and momentum, then requiring wavefunctions to be periodic in both position and momentum space, possibly up to a phase. This produces a Hilbert space of finite dimension N with an effective, rational Planck's constant of $\hbar = 1/N$. A basis for the Hilbert space \mathcal{H} is given by delta-localized position eigenstates $|q_j\rangle$ for $q_j = j/N$ with j understood modulo N . The unitary map U on \mathcal{H} corresponding to the classical cat map is computed by taking the semiclassical approximation of the propagator

(also known as the stationary phase approximation or the Van Vleck formula) in position space to be exact. For the map (A.3), the matrix elements are given by

$$\begin{aligned} \langle q_k | U | q_j \rangle &= \sqrt{\frac{A_{12}}{N}} \exp \left\{ \frac{i\pi}{A_{12}N} (A_{11}j^2 - 2jk + A_{22}k^2) + \frac{i\kappa N}{2\pi} \sin \left(\frac{2\pi j}{N} \right) \right\} \\ &\times G \left(N' A_{11}, A'_{12}, \frac{2(A_{11}j - k)}{\gcd(N, A_{12})} \right) \end{aligned} \quad (\text{A.4})$$

where $N' = N/\gcd(N, A_{12})$, $A'_{12} = A_{12}/\gcd(N, A_{12})$, and G is a Gauss average function

$$G(a, b, c) = \lim_{M \rightarrow \infty} \frac{1}{2M} \sum_{m=-M}^M \exp \left\{ \frac{i\pi}{b} (am^2 + cm) \right\} \quad (\text{A.5})$$

for coprime integers a and b . The G function is evaluated in Ref. [41].

For further detail on the quantization of the cat map, see Ref. [42, 68, 69]. The total wavefunctions need only be periodic up to a phase, the effects of which are discussed in Ref. [70]. The cat map unitary also has quantum symmetries with no classical counterpart, as constructed in Ref. [44, 45]. The semiclassical limit of quantum maps is well-studied [66, 68, 71–76]. Basics of quantization and semiclassics for quantum maps on the torus are reviewed in Ref. [57]. There are alternative quantization schemes as well, such as a quadratic kick [77]. One may also remove the constraints on wavefunctions and the Hilbert space, and instead perform a noncommutative deformation at the algebraic level. This allows for any Planck's constant $\hbar \in \mathbb{R}$, but the resulting Hilbert space is infinite dimensional for irrational \hbar [78]. The AFL entropy h_{AFL} has been computed for this algebraic quantum cat map and matches the classical KS value [79].

A.3 Proof of Anticommutation

The following is adapted from Appx. B of Esposti and Winn (EW) [24], which proves that when the Hilbert space dimension N is divisible by 4,

$$U_{kj} = (-1)^{j-k} U_{N/2-k, N/2-j} \quad (\text{A.6})$$

where U is the unperturbed⁹ quantum cat map unitary. This property proves the unitary W defined in (3.4) commutes with U by way of the relation

$$(W^\dagger U W)_{kj} = (-1)^{j-k} U_{N/2-k, N/2-j} \quad (\text{A.7})$$

What we show here is that when N is even but not divisible by 4, it is possible to instead have the relation

$$U_{kj} = (-1)^{j-k+1} U_{N/2-k, N/2-j} \quad (\text{A.8})$$

which implies W and U *anticommute*. The calculation differs from that of EW by occasional factors of -1 , which we tally below. Before we begin, note the cat map matrix is always

⁹For particular choices of perturbation, such as our choice of (A.3), W commutes with the quantized perturbation and so the commutation results apply to the perturbed map as well [24].

of a chessboard form

$$A = \begin{pmatrix} \text{odd} & \text{even} \\ \text{even} & \text{odd} \end{pmatrix} \text{ or } A = \begin{pmatrix} \text{even} & \text{odd} \\ \text{odd} & \text{even} \end{pmatrix} \quad (\text{A.9})$$

and we use the notation $N' = N/\gcd(N, A_{12})$ and $A'_{12} = A_{12}/\gcd(N, A_{12})$. N is even but not divisible by 4 throughout the calculation.

Case $N'A_{11}A'_{12}$ even. The calculations of EW follow unchanged until the A_{11} even case of equations (EW.B.14–15). With A_{11} even, A_{12} is odd and N' is even. The factor under consideration is

$$\exp\left(-\pi\frac{NA_{11}}{4A_{12}}\ell A'_{12}\right) = \exp\left(-\frac{\pi}{4}N'A_{11}\ell\right) \quad (\text{A.10})$$

which is +1 only if $4|A_{11}$ or $2|\ell$, and is -1 otherwise. The integer ℓ is defined by

$$\begin{aligned} \ell A'_{12} &= (1 - A_{22} + A_{12}A_{21} + mA'_{12}(A_{11} - 1))^2 - (1 - A_{22})^2 \\ &= m^2 A'_{12}{}^2 (A_{11} - 1)^2 + A_{12}^2 A_{21}^2 + 2qA'_{12} \\ &= (m^2 A'_{12}(A_{11} - 1)^2 + A_{12}A_{21}^2 \gcd(N, A_{12}) + 2q)A'_{12} \end{aligned} \quad (\text{A.11})$$

where

$$q = (1 - A_{22})A_{21} \gcd(N, A_{12}) + m(A_{11} - 1)(1 - A_{22} + A_{12}A_{21}) \quad (\text{A.12})$$

Note $A'_{12}(A_{11} - 1)^2$ and $A_{12}A_{21}^2 \gcd(N, A_{12})$ are odd, so the parity of ℓ is opposite that of m . The integer m is itself defined by

$$N'(N'A_{11} \setminus A'_{12}) = A_{22} + mA'_{12} \quad (\text{A.13})$$

where $x \setminus y$ is the inverse of x modulo y ($N'A_{11}$ and A'_{12} are coprime). N' and A_{22} are even and A'_{12} is odd, so m must be even. Thus, ℓ is always odd. The exponential factor is then -1 if A_{11} is even but not divisible by 4. Otherwise (including the A_{11} odd case from EW), the factor is +1.

The next change is at equation (EW.B.17), with the factor

$$\exp\left(-\frac{\pi}{4}N(2 - A_{22})A_{21}\right). \quad (\text{A.14})$$

Observe N is even but not divisible by 4 and $(2 - A_{22})A_{21}$ is even, so the expression simplifies to +1 if $4|(2 - A_{22})A_{21}$ and -1 otherwise.

Case $N'A_{11}A'_{12}$ odd. Here, each factor in $N'A_{11}A'_{12}$ is odd so we are in the $\mathbf{A} = \begin{pmatrix} \text{odd} & \text{even} \\ \text{even} & \text{odd} \end{pmatrix}$ case. The computation of EW follows unchanged until equation (EW.B.25), where the factor (A.14) appears again.¹⁰ This time, A_{21} is even and $(2 - A_{22})$ is odd, so the factor is +1 if $4|A_{21}$ and -1 otherwise.

The final change from EW occurs at equation (EW.B.26) in the expression

$$\exp\left(\frac{\pi}{2}\gcd(N, A_{12})\right). \quad (\text{A.15})$$

¹⁰To be clear, expression (A.14) appears in the expansion of $\exp(-\pi NA_{11}(1 - A_{22})^2/4A_{12})$, which also appears in the algebra preceding (EW.B.25).

Note N' is odd while $N = N' \gcd(N, A_{12})$ is even but not divisible by 4. Thus, $\gcd(N, A_{12})$ is also even but not divisible by 4 and this factor is always -1 .

Summary. Let us simplify the above conditions by tallying the possible -1 factors. Taking A_{11} as even places us in the $N'A_{11}A'_{12}$ even case with A_{22} even as well. We get a factor of -1 from (A.10) if $4 \nmid A_{11}$ and another from (A.14) if $4|A_{22}$.

Now we take A_{11} to be odd. We get a factor of -1 from (A.14) if $4 \nmid A_{21}$. If $4 \nmid A_{12}$, we are in the $N'A_{11}A'_{12}$ odd case and get a -1 factor from (A.15). If $4|A_{12}$, we are in the $N'A_{11}A'_{12}$ even case where no such factor appears.

To summarize, if A_{11} is even, then W and U commute if and only if 4 divides exactly one of A_{11} or A_{22} . If A_{11} is odd, then W and U commute if and only if 4 divides both or neither of A_{12} and A_{21} . In all other cases, we are left with an overall factor of -1 which yields equation (A.8), making W and U anticommute. These results are shown as a table in Fig. 7. The maps we chose for numerics, $\mathbf{A} = \begin{pmatrix} 6 & 5 \\ 7 & 6 \end{pmatrix}$ and $\mathbf{A} = \begin{pmatrix} 2 & 1 \\ 3 & 2 \end{pmatrix}$, satisfy the anticommutation conditions.

A_{11} even			A_{11} odd		
	$4 A_{11}$	$4 \nmid A_{11}$		$4 A_{12}$	$4 \nmid A_{12}$
$4 A_{22}$	AC	C	$4 A_{21}$	C	AC
$4 \nmid A_{22}$	C	AC	$4 \nmid A_{21}$	AC	C

Figure 7: The conditions on the classical cat matrix \mathbf{A} for the corresponding quantum cat map unitary U to commute or anticommute with W as defined by equation (3.4), given the dimension of the Hilbert space N is even but not divisible by 4. Here, “C” means commuting ($[W, U] = 0$) and “AC” means anticommuting ($\{W, U\} = 0$).

A.4 The R and W Algebra

Here, we compute the representation described in Sect. 6 of the non-Abelian algebra \mathcal{A} generated by the cat R and W unitaries, defined as

$$R|q_j\rangle = \omega_s^j |q_j\rangle \tag{A.16}$$

$$W|q_j\rangle = (-1)^j |q_{\frac{N}{2}-j}\rangle \tag{A.17}$$

where $\omega_s = \exp(i2\pi/s)$ is a root of unity and N is the dimension of the Hilbert space. For simplicity, we take s to be an odd prime, as it is for the cat map (3.6), so that ω_s^n is a primitive s th root of unity for $n \not\equiv 0 \pmod{s}$. For both R and W to be symmetries, we require $N = sM$ with M divisible by 4.

First, note that R only distinguishes the indices j modulo s . In other words, the n th power R^n can be understood modulo s , with $R^s = R^0 = \mathbf{1}$. The W operator has $W^2 = \mathbf{1}$ and has a nontrivial relation to R due to

$$\frac{N}{2} - j \equiv -j \pmod{s} \tag{A.18}$$

which leads directly to the relation

$$WR = R^{-1}W. \quad (\text{A.19})$$

Therefore, a general operator $A \in \mathcal{A}$ admits the form

$$A = \sum_{n=0}^{s-1} (x_n \mathbb{1} + y_n W) R^n \quad (\text{A.20})$$

for some complex coefficients x_n and y_n .

For completeness, we compute the center of the algebra, although this is not strictly necessary to find the representation (6.1). The identity $\sum_{n=0}^{s-1} \omega_s^n = 0$ will prove useful here. Given an operator Z

$$Z = \sum_{m=0}^{s-1} (\alpha_m \mathbb{1} + \beta_m W) R^m \quad (\text{A.21})$$

in the center \mathcal{Z} of \mathcal{A} , the commutator with A must vanish. We directly compute

$$\begin{aligned} [Z, A] = \sum_{n,m} \{ & \beta_m y_n (R^{n-m} - R^{m-n}) + \beta_m x_n W (R^{m+n} - R^{m-n}) \\ & + \alpha_m y_n W (R^{n-m} - R^{m+n}) \} \end{aligned} \quad (\text{A.22})$$

which gives us the conditions

$$0 = \sum_{n,m} \beta_m y_n (\omega_s^{n-m} - \omega_s^{m-n}) \quad (\text{A.23})$$

$$0 = \sum_{n,m} \{ \beta_m x_n (\omega_s^{m+n} - \omega_s^{m-n}) + \alpha_m y_n (\omega_s^{n-m} - \omega_s^{m+n}) \} \quad (\text{A.24})$$

for arbitrary x_n and y_n . Relation (A.23) constrains β_m to be an m -independent (possibly zero) constant, so that the sum over m vanishes for each term independently. This also means the first term in (A.24) is zero. The second term constrains α_m to be symmetric: $\alpha_m = \alpha_{-m}$. The center is then spanned by $R^n + R^{-n}$ for $n = 0, \dots, s-1$ and $W\Delta$ where Δ is the projector

$$\Delta = \frac{1}{s} \sum_{n=0}^{s-1} R^n \quad (\text{A.25})$$

$$\Rightarrow \Delta |q_j\rangle = \delta(j \equiv 0 \pmod{s}) |q_j\rangle \quad (\text{A.26})$$

The irreps of the center provide the direct sum decomposition (6.1). Observe \mathcal{Z} is only sensitive to the index j modulo s . The $j \equiv 0 \pmod{s}$ subspace ($R + R^{-1} = 2$) contains two irreps: the eigenspaces $W\Delta = +1$ and $W\Delta = -1$. The $j \not\equiv 0 \pmod{s}$ subspace ($W\Delta = 0$) splits into $\frac{s-1}{2}$ irreps corresponding to the remaining distinct eigenvalues of $R + R^{-1}$, with j and $-j \pmod{s}$ in the same representation.

To better understand the representation, consider the action of the generators for $N = 20$ and $s = 5$, as shown in Fig. 8. The lines show the indices that swap under W , with

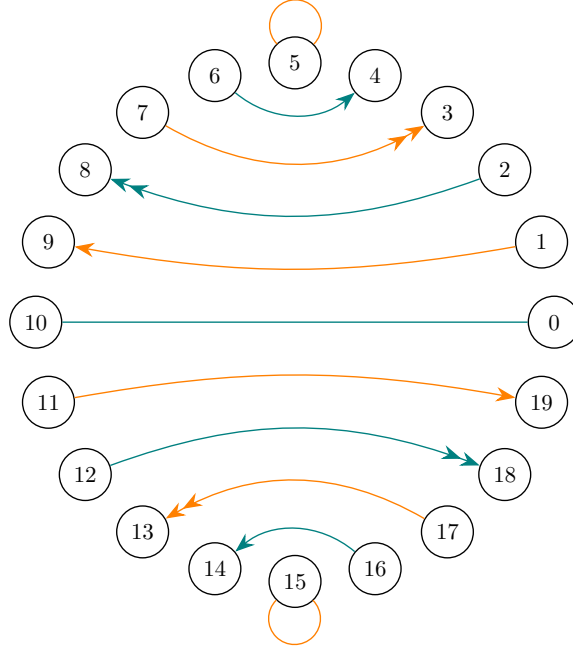


Figure 8: Graphical representation of the action of R and W on the quantum cat map Hilbert space of dimension $N = 20$. The lines notate the action of W and the arrow heads notate the action of R as described in the text.

teal corresponding to no phase and orange corresponding to a factor of -1 upon swapping. The lines with no heads connect to the $R = +1$ indices, which are 0 modulo 5. The single-headed arrows point from 1 to -1 modulo 5, and the double-headed arrows point from 2 to -2 modulo 5. Thus, the algebra acts on $(|q_1\rangle, -|q_9\rangle)$ the same as it does on $(|q_6\rangle, |q_4\rangle)$, $(|q_{11}\rangle, -|q_{19}\rangle)$, and $(|q_{16}\rangle, |q_{14}\rangle)$.

This motivates the following tensor product structure:

$$\begin{aligned} |j \uparrow\rangle \otimes |k\rangle_s &:= |q_{j+ks}\rangle \\ |j \downarrow\rangle \otimes |k\rangle_s &:= (-1)^{j+ks} |q_{\frac{N}{2}-j-ks}\rangle \end{aligned} \quad (\text{A.27})$$

for $j = 0, \dots, \frac{s-1}{2}$ and k is an index taken modulo $M = N/s$. These vectors span the Hilbert space but double count the following states:

$$\begin{aligned} |0 \uparrow\rangle \left| \frac{M}{4} \right\rangle_s &= (-1)^{\frac{M}{4}} |0 \downarrow\rangle \left| \frac{M}{4} \right\rangle_s \\ |0 \uparrow\rangle \left| -\frac{M}{4} \right\rangle_s &= (-1)^{\frac{M}{4}} |0 \downarrow\rangle \left| -\frac{M}{4} \right\rangle_s \end{aligned} \quad (\text{A.28})$$

The generators of \mathcal{A} act as

$$\begin{aligned} R |j \uparrow\rangle |k\rangle_s &= \omega_s^j |j \uparrow\rangle |k\rangle_s \\ R |j \downarrow\rangle |k\rangle_s &= \omega_s^{-j} |j \downarrow\rangle |k\rangle_s \end{aligned} \quad (\text{A.29})$$

$$\begin{aligned} W |j \uparrow\rangle |k\rangle_s &= |j \downarrow\rangle |k\rangle_s \\ W |j \downarrow\rangle |k\rangle_s &= |j \uparrow\rangle |k\rangle_s \end{aligned} \quad (\text{A.30})$$

The algebra acts trivially on the $|k\rangle_s$ space, but nontrivially on the $|j, \uparrow/\downarrow\rangle$ space. The double-counted states (A.28) are eigenstates of W with eigenvalue $(-1)^{\frac{M}{4}}$.

Now the subspaces from decomposition (6.1) are clear:

$$W\Delta = (-1)^{\frac{M}{4}} : \mathcal{H}_0^+ = \text{span}\{|0 \uparrow\rangle |k\rangle_s + (-1)^{\frac{M}{4}} |0 \downarrow\rangle |k\rangle_s \mid k = -\frac{M}{4}, \dots, \frac{M}{4}\} \quad (\text{A.31})$$

$$W\Delta = (-1)^{\frac{M}{4}+1} : \mathcal{H}_0^- = \text{span}\{|0 \uparrow\rangle |k\rangle_s - (-1)^{\frac{M}{4}} |0 \downarrow\rangle |k\rangle_s \mid k = 1 - \frac{M}{4}, \dots, \frac{M}{4} - 1\} \quad (\text{A.32})$$

$$\begin{aligned} W\Delta = 0 : & \text{ Splits into representations } \mathcal{H}_j = \mathcal{K}_j \otimes \mathcal{K}'_j \text{ where} \\ & \mathcal{K}_j = \text{span}\{|j \uparrow\rangle, |j \downarrow\rangle\} \\ & \mathcal{K}'_j = \text{span}\{|k\rangle_s \mid k = 0, \dots, M-1\} \\ & \text{for } j = 1, \dots, \frac{s-1}{2} \end{aligned} \quad (\text{A.33})$$

Decomposing the Hilbert space as

$$\mathcal{H} = \mathcal{H}_0^+ \oplus \mathcal{H}_0^- \oplus \bigoplus_{j=1}^{\frac{s-1}{2}} \mathcal{K}_j \otimes \mathcal{K}'_j \quad (\text{A.34})$$

the algebra takes the form

$$\mathcal{A} = \mathbb{C} \mathbf{1}_{\frac{M}{2}+1} \oplus \mathbb{C} \mathbf{1}_{\frac{M}{2}-1} \oplus \bigoplus_{j=1}^{\frac{s-1}{2}} \mathcal{L}(\mathbb{C}^2) \otimes \mathbf{1}_M \quad (\text{A.35})$$

Picking $(|j \uparrow\rangle, |j \downarrow\rangle)$ as the basis for the two-dimensional irreps \mathcal{K}_j , the generators are matrices

$$R = \mathbf{1}_{\frac{M}{2}+1} \oplus \mathbf{1}_{\frac{M}{2}-1} \oplus \bigoplus_{j=1}^{\frac{s-1}{2}} \begin{pmatrix} \omega_s^j & 0 \\ 0 & \omega_s^{-j} \end{pmatrix} \otimes \mathbf{1}_M \quad (\text{A.36})$$

$$W = (-1)^{\frac{M}{4}} \mathbf{1}_{\frac{M}{2}+1} \oplus (-1)^{\frac{M}{4}+1} \mathbf{1}_{\frac{M}{2}-1} \oplus \bigoplus_{j=1}^{\frac{s-1}{2}} \begin{pmatrix} 0 & 1 \\ 1 & 0 \end{pmatrix} \otimes \mathbf{1}_M \quad (\text{A.37})$$

As a sanity check, the algebra has $1 + 1 + \frac{s-1}{2} \times 2^2 = 2s$ complex degrees of freedom from the decomposition into irreps (A.35), which matches the number of complex parameters in the expansion of a general operator (A.20).

B Proof of Theorem 1 in System and Purifier Space

Proof. After t time steps of the measurement channel, the state of the system and purifier is

$$\begin{aligned}
\sigma[(U\mathcal{X})^t] &= \sum_i |UX^{i_t} \dots UX^{i_1} \sqrt{\rho}\rangle \langle\langle UX^{i_t} \dots UX^{i_1} \sqrt{\rho}| \\
&= \sum_i \left| \bigoplus_{\lambda} U_{\lambda} X_{\lambda}^{i_t} \dots U_{\lambda} X_{\lambda}^{i_1} \sqrt{p_{\lambda} \rho_{\lambda}} \right\rangle \langle\langle \bigoplus_{\mu} U_{\mu} X_{\mu}^{i_t} \dots U_{\mu} X_{\mu}^{i_1} \sqrt{p_{\mu} \rho_{\mu}} \left| \right. \\
&= \sum_i \left(\bigoplus_{\lambda} \sqrt{p_{\lambda}} |U_{\lambda} X_{\lambda}^{i_t} \dots U_{\lambda} X_{\lambda}^{i_1} \sqrt{\rho_{\lambda}}\rangle \right) \\
&\quad \otimes \left(\bigoplus_{\mu} \sqrt{p_{\mu}} \langle\langle U_{\mu} X_{\mu}^{i_t} \dots U_{\mu} X_{\mu}^{i_1} \sqrt{\rho_{\mu}} \left| \right. \right)
\end{aligned} \tag{B.1}$$

To write this in a more transparent way, we can define

$$\mathcal{S}_{\lambda\mu} = \sum_i \sqrt{p_{\lambda} p_{\mu}} |U_{\lambda} X_{\lambda}^{i_t} \dots U_{\lambda} X_{\lambda}^{i_1} \sqrt{\rho_{\lambda}}\rangle \langle\langle U_{\mu} X_{\mu}^{i_t} \dots U_{\mu} X_{\mu}^{i_1} \sqrt{\rho_{\mu}} \left| \right. \tag{B.2}$$

which is a map $\mathcal{H}_{\mu}^{\otimes 2} \mapsto \mathcal{H}_{\lambda}^{\otimes 2}$. If we abuse notation and use $\mathcal{S}_{\lambda\mu}$ to refer additionally to the respective map from $\mathcal{H}_{\mu}^{\otimes 2}$ to itself (with support on $\mathcal{H}_{\mu}^{\otimes 2}$ and image in $\mathcal{H}_{\lambda}^{\otimes 2}$), we can write $\sigma = \sum_{\lambda\mu} \mathcal{S}_{\lambda\mu}$. This means σ is a density matrix on $\bigoplus_{\lambda} \mathcal{H}_{\lambda}^{\otimes 2} \subseteq \mathcal{H}^{\otimes 2}$ with $\mathcal{S}_{\lambda\mu}$ as blocks:

$$\sigma[(U\mathcal{X})^t] = \begin{pmatrix} \boxed{\mathcal{S}_{\lambda_1 \lambda_1}} & \cdots & \boxed{\mathcal{S}_{\lambda_1 \lambda_n}} \\ \vdots & \ddots & \vdots \\ \boxed{\mathcal{S}_{\lambda_n \lambda_1}} & \cdots & \boxed{\mathcal{S}_{\lambda_n \lambda_n}} \end{pmatrix} \text{ on } \bigoplus_{\lambda} \mathcal{H}_{\lambda}^{\otimes 2} \tag{B.3}$$

The diagonal blocks can be written as

$$\begin{aligned}
\mathcal{S}_{\lambda\lambda} &= p_{\lambda} \sum_i |U_{\lambda} X_{\lambda}^{i_t} \dots U_{\lambda} X_{\lambda}^{i_1} \sqrt{\rho_{\lambda}}\rangle \langle\langle U_{\lambda} X_{\lambda}^{i_t} \dots U_{\lambda} X_{\lambda}^{i_1} \sqrt{\rho_{\lambda}} \left| \right. \\
&= p_{\lambda} \sigma_{\lambda} [(U_{\lambda} \mathcal{X}_{\lambda})^t]
\end{aligned} \tag{B.4}$$

where $\sigma_{\lambda} [(U_{\lambda} \mathcal{X}_{\lambda})^t]$ is the state of the restricted density matrix ρ_{λ} and its purifier after t time steps. Note the block-diagonal part of σ is itself a density matrix of the form

$$\varrho = \bigoplus_{\lambda} \mathcal{S}_{\lambda\lambda} = \bigoplus_{\lambda} p_{\lambda} \sigma_{\lambda} [(U_{\lambda} \mathcal{X}_{\lambda})^t] \tag{B.5}$$

with von Neumann entropy

$$S(\varrho) = \sum_{\lambda} p_{\lambda} S(\sigma_{\lambda} [(U_{\lambda} \mathcal{X}_{\lambda})^t]) + H_S(\{p_{\lambda}\}) \tag{B.6}$$

since the σ_λ have orthogonal support. Now we recall that a Hermitian matrix majorizes the matrix given by its block-diagonal part [80], so $\sigma \succ \varrho$. This implies $S(\sigma) \leq S(\varrho)$ [50], and so we have

$$S(\sigma[(U\mathcal{X})^t]) \leq \sum_{\lambda} p_{\lambda} S(\sigma_{\lambda}[(U_{\lambda}\mathcal{X}_{\lambda})^t]) + H_S(\{p_{\lambda}\}) \quad (\text{B.7})$$

as desired.

For the equality case, we now take the Kraus operators in \mathcal{X} to have support on exactly one charge sector each. Due to equation (4.6), the nonzero terms of $\mathcal{S}_{\lambda\mu}$ require $\mathbf{i} \sim \lambda$ and $\mathbf{i} \sim \mu$ simultaneously, meaning $\mathcal{S}_{\lambda\mu}$ vanishes for $\lambda \neq \mu$. Thus, σ is equal to its block-diagonal part ϱ , and in particular $S(\sigma) = S(\varrho)$ as desired. \square

References

- [1] P. Walters, *An Introduction to Ergodic Theory*. Springer New York, 1982.
- [2] A. Connes and E. Størmer, *Entropy for automorphisms of II₁ von Neumann algebras*, *Acta Mathematica* **134** (1975), no. 1 289–306.
- [3] A. Connes, H. Narnhofer, and W. Thirring, *Dynamical entropy of C* algebras and von Neumann algebras*, *Communications in Mathematical Physics* **112** (1987), no. 4 691–719.
- [4] R. Alicki and M. Fannes, *Defining quantum dynamical entropy*, *Letters in Mathematical Physics* **32** (1994), no. 1 75–82.
- [5] W. Słomczyński and K. Życzkowski, *Quantum chaos: An entropy approach*, *Journal of Mathematical Physics* **35** (1994), no. 11 5674–5700.
- [6] D. Voiculescu, *Dynamical approximation entropies and topological entropy in operator algebras*, *Communications in Mathematical Physics* **170** (1995), no. 2 249–281.
- [7] W. Słomczyński and A. Szczepanek, *Quantum Dynamical Entropy, Chaotic Unitaries and Complex Hadamard Matrices*, *IEEE Transactions on Information Theory* **63** (2017), no. 12 7821–7831.
- [8] H. Gharibyan, M. Hanada, B. Swingle, and M. Tezuka, *Quantum lyapunov spectrum*, *Journal of High Energy Physics* **2019** (2019), no. 4 82.
- [9] T. Goldfriend and J. Kurchan, *Quantum kolmogorov-sinai entropy and pesin relation*, *Phys. Rev. Res.* **3** (Jun, 2021) 023234.
- [10] G. Maier, A. Schäfer, and S. Waeber, *Holographic kolmogorov-sinai entropy and the quantum lyapunov spectrum*, *Journal of High Energy Physics* **2022** (2022), no. 1 165.
- [11] N. Dowling and K. Modi, *Operational metric for quantum chaos and the corresponding spatiotemporal-entanglement structure*, *PRX Quantum* **5** (Feb, 2024) 010314.
- [12] R. Alicki, D. Makowiec, and W. Miklaszewski, *Quantum Chaos in Terms of Entropy for a Periodically Kicked Top*, *Physical Review Letters* **77** (1996), no. 5 838–841.
- [13] R. Alicki, *Quantum Ergodic Theory and Communication Channels*, *Open Systems & Information Dynamics* **4** (1997), no. 1 53–69.
- [14] R. Alicki, *Information-theoretical meaning of quantum-dynamical entropy*, *Physical Review A* **66** (2002), no. 5 052302.

- [15] R. Alicki, A. Loziński, P. Pakoński, and K. Życzkowski, *Quantum dynamical entropy and decoherence rate*, *Journal of Physics A: Mathematical and General* **37** (2004), no. 19 5157.
- [16] J. Cotler, C.-M. Jian, X.-L. Qi, and F. Wilczek, *Superdensity operators for spacetime quantum mechanics*, *Journal of High Energy Physics* **2018** (2018), no. 9 93.
- [17] O. Bohigas, M. J. Giannoni, and C. Schmit, *Characterization of chaotic quantum spectra and universality of level fluctuation laws*, *Phys. Rev. Lett.* **52** (Jan, 1984) 1–4.
- [18] F. Chen and P. Fang, *System Symmetry and the Classification of Out-of-Time-Ordered Correlator Dynamics in Quantum Chaos*, [arXiv:2410.04712](https://arxiv.org/abs/2410.04712).
- [19] V. Balasubramanian, R. N. Das, J. Erdmenger, and Z.-Y. Xian, *Chaos and integrability in triangular billiards*, [arXiv:2407.11114](https://arxiv.org/abs/2407.11114).
- [20] P. Bracken, *Introductory chapter: Dynamical symmetries and quantum chaos*, in *Research Advances in Chaos Theory* (P. Bracken, ed.), ch. 1. IntechOpen, Rijeka, 2020.
- [21] A. Pandey, R. Ramaswamy, and P. Shukla, *Symmetry breaking in quantum chaotic systems*, *Pramana* **41** (1993), no. 1 L75–L81.
- [22] K. Sharma, H. Sahu, and S. Mukerjee, *Quantum chaos in PT symmetric quantum systems*, [arXiv:2401.07215](https://arxiv.org/abs/2401.07215).
- [23] J. de la Cruz, S. Lerma-Hernández, and J. G. Hirsch, *Quantum chaos in a system with high degree of symmetries*, *Phys. Rev. E* **102** (Sep, 2020) 032208.
- [24] M. D. Esposti and B. Winn, *The quantum perturbed cat map and symmetry*, *Journal of Physics A: Mathematical and General* **38** (2005), no. 26 5895–5912.
- [25] X. Chen and T. Zhou, *Operator scrambling and quantum chaos*, [arXiv:1804.08655](https://arxiv.org/abs/1804.08655).
- [26] I. García-Mata, M. Saraceno, R. A. Jalabert, A. J. Roncaglia, and D. A. Wisniacki, *Chaos Signatures in the Short and Long Time Behavior of the Out-of-Time Ordered Correlator*, *Physical Review Letters* **121** (2018), no. 21 210601.
- [27] S. Moudgalya, T. Devakul, C. W. Von Keyserlingk, and S. L. Sondhi, *Operator spreading in quantum maps*, *Physical Review B* **99** (2019), no. 9 094312.
- [28] L. Nie, *Operator Growth and Symmetry-Resolved Coefficient Entropy in Quantum Maps*, [arXiv:2111.08729](https://arxiv.org/abs/2111.08729).
- [29] G. Lindblad, *Non-Markovian quantum stochastic processes and their entropy*, *Communications in Mathematical Physics* **65** (1979), no. 3 281–294.
- [30] G. Lindblad, *Quantum entropy and quantum measurements*, in *Quantum Aspects of Optical Communications* (C. Bendjaballah, O. Hirota, and S. Reynaud, eds.), (Berlin, Heidelberg), pp. 79–80, Springer, 1991.
- [31] M. A. Nielsen and I. L. Chuang, *Quantum Computation and Quantum Information: 10th Anniversary Edition*. Cambridge University Press, 2010.
- [32] M. M. Wilde, *From Classical to Quantum Shannon Theory*. 2021.
- [33] B. Schumacher, *Sending entanglement through noisy quantum channels*, *Physical Review A* **54** (1996), no. 4 2614–2628.
- [34] J. C. Bridgeman and C. T. Chubb, *Hand-waving and interpretive dance: An introductory course on tensor networks*, *Journal of Physics A: Mathematical and Theoretical* **50** (2017), no. 22 223001.

- [35] J. Biamonte, *Lectures on Quantum Tensor Networks*, [arXiv:1912.10049](https://arxiv.org/abs/1912.10049).
- [36] R. Alicki, J. Andries, M. Fannes, and P. Tuijls, *An algebraic approach to the kolmogorov-sinai entropy*, *Reviews in Mathematical Physics* **08** (1996), no. 02 167–184.
- [37] R. Alicki, *Quantum mechanical tools in applications to classical dynamical systems*, *Phys. Rev. Lett.* **81** (Sep, 1998) 2040–2043.
- [38] F. Benatti, V. Cappellini, M. De Cock, M. Fannes, and D. Vanpeteghem, *Classical Limit of Quantum Dynamical Entropies*, *Reviews in Mathematical Physics* **15** (2003), no. 08 847–875, [[quant-ph/0308069](https://arxiv.org/abs/quant-ph/0308069)].
- [39] D. Shepelyansky, *Ehrenfest time and chaos*, *Scholarpedia* **15** (2020), no. 9 55031.
- [40] V. I. Arnol'd, *Ergodic Problems of Classical Mechanics*. The Mathematical Physics Monograph Series. Benjamin, New York, 1968.
- [41] J. Hannay and M. Berry, *Quantization of linear maps on a torus-fresnel diffraction by a periodic grating*, *Physica D: Nonlinear Phenomena* **1** (1980), no. 3 267–290.
- [42] M. D. Esposti, *Quantization of the orientation preserving automorphisms of the torus*, *Annales de l'I.H.P. Physique théorique* **58** (1993), no. 3 323–341.
- [43] M. B. de Matos and A. M. O. de Almeida, *Quantization of Anosov Maps*, *Annals of Physics* **237** (1993), no. 1 46–65.
- [44] P. Kurlberg and Z. Rudnick, *Hecke theory and equidistribution for the quantization of linear maps of the torus*, *Duke Mathematical Journal* **103** (2000), no. 1 47–77.
- [45] J. P. Keating and F. Mezzadri, *Pseudo-symmetries of Anosov maps and spectral statistics*, *Nonlinearity* **13** (2000), no. 3 747–775.
- [46] A. Bäcker, *Numerical Aspects of Eigenvalue and Eigenfunction Computations for Chaotic Quantum Systems*, in *The Mathematical Aspects of Quantum Maps* (M. D. Esposti and S. Graffi, eds.), vol. 618, pp. 91–144. Springer, Berlin, Heidelberg, 2003.
- [47] S. Nonnenmacher, *Spectral properties of noisy classical and quantum propagators*, *Nonlinearity* **16** (2003), no. 5 1685.
- [48] I. García-Mata, M. Saraceno, and M. E. Spina, *Classical Decays in Decoherent Quantum Maps*, *Physical Review Letters* **91** (2003), no. 6 064101.
- [49] I. García-Mata, R. A. Jalabert, and D. A. Wisniacki, *Out-of-time-order correlations and quantum chaos*, *Scholarpedia* **18** (2023), no. 4 55237.
- [50] M. A. Nielsen, *An Introduction to Majorization and Its Applications to Quantum Mechanics*. University of Queensland, 2002.
- [51] https://github.com/ericdschultz/AFL_numerics.
- [52] C. Bény and F. Richter, *Algebraic approach to quantum theory: A finite-dimensional guide*, [arXiv:1505.03106](https://arxiv.org/abs/1505.03106).
- [53] D. Harlow, *The Ryu–Takayanagi Formula from Quantum Error Correction*, *Communications in Mathematical Physics* **354** (2017), no. 3 865–912.
- [54] S. Moudgalya and O. I. Motrunich, *Hilbert Space Fragmentation and Commutant Algebras*, *Physical Review X* **12** (2022), no. 1 011050.
- [55] S. Moudgalya and O. I. Motrunich, *From symmetries to commutant algebras in standard Hamiltonians*, *Annals of Physics* **455** (2023) 169384.

- [56] M. Fannes and P. Tuyls, *A continuity property of quantum dynamical entropy*, *Infinite Dimensional Analysis, Quantum Probability and Related Topics* **02** (1999), no. 04 511–527.
- [57] M. D. Esposti and S. Graffi, *Mathematical Aspects of Quantum Maps*, in *The Mathematical Aspects of Quantum Maps* (M. D. Esposti and S. Graffi, eds.), pp. 49–90. Springer, Berlin, Heidelberg, 2003.
- [58] M. Axenides, E. Floratos, and S. Nicolis, *The quantum cat map on the modular discretization of extremal black hole horizons*, *The European Physical Journal C* **78** (2018), no. 5 412.
- [59] J. M. Magan and Q. Wu, *Two types of quantum chaos: testing the limits of the Bohigas-Giannoni-Schmit conjecture*, [arXiv:2411.08186](https://arxiv.org/abs/2411.08186).
- [60] T. Hudetz, *Quantum dynamical entropy revisited*, *Banach Center Publications* **43** (1998), no. 1 241–251.
- [61] F. Benatti, T. Hudetz, and A. Knauf, *Quantum Chaos and Dynamical Entropy*, *Communications in Mathematical Physics* **198** (1998), no. 3 607–688.
- [62] R. Alicki and H. Narnhofer, *Comparison of dynamical entropies for the noncommutative shifts*, *Letters in Mathematical Physics* **33** (1995), no. 3 241–247.
- [63] L. Accardi, M. Ohya, and N. Watanabe, *Note on quantum dynamical entropies*, *Reports on Mathematical Physics* **38** (1996), no. 3 457–469.
- [64] P. Tuyls, *Comparing quantum dynamical entropies*, *Banach Center Publications* **43** (1998), no. 1 411–420.
- [65] M. Fannes and B. Haegeman, *Quantum dynamical entropies for classical stochastic systems*, *Reports on Mathematical Physics* **52** (2003), no. 1 151–165, [[math-ph/0206037](https://arxiv.org/abs/math-ph/0206037)].
- [66] P. A. Boasman and J. P. Keating, *Semiclassical Asymptotics of Perturbed Cat Maps*, *Proceedings: Mathematical and Physical Sciences* **449** (1995), no. 1937 629–653, [[52684](https://arxiv.org/abs/math-ph/9505022)].
- [67] M. V. Berry, N. L. Balazs, M. Tabor, and A. Voros, *Quantum maps*, *Annals of Physics* **122** (1979), no. 1 26–63.
- [68] M. D. Esposti, S. Graffi, and S. Isola, *Classical limit of the quantized hyperbolic toral automorphisms*, *Communications in Mathematical Physics* **167** (1995), no. 3 471–507.
- [69] S. De Bièvre, M. D. Esposti, and R. Giachetti, *Quantization of a class of piecewise affine transformations on the torus*, *Communications in Mathematical Physics* **176** (1996), no. 1 73–94.
- [70] J. P. Keating, F. Mezzadri, and J. M. Robbins, *Quantum boundary conditions for torus maps*, *Nonlinearity* **12** (1999), no. 3 579–591.
- [71] B. Eckhardt, *Exact eigenfunctions for a quantised map*, *Journal of Physics A: Mathematical and General* **19** (1986), no. 10 1823.
- [72] J. P. Keating, *The cat maps: Quantum mechanics and classical motion*, *Nonlinearity* **4** (1991), no. 2 309–341.
- [73] A. Bouzouina and S. De Bièvre, *Equipartition of the eigenfunctions of quantized ergodic maps on the torus*, *Communications in Mathematical Physics* **178** (1996), no. 1 83–105.
- [74] P. Kurlberg and Z. Rudnick, *On Quantum Ergodicity for Linear Maps of the Torus*, *Communications in Mathematical Physics* **222** (2001), no. 1 201–227.

- [75] M. Horvat, T. Prosen, and M. D. Esposti, *Quantum–classical correspondence on compact phase space*, *Nonlinearity* **19** (2006), no. 6 1471–1493.
- [76] M. Horvat and M. D. Esposti, *The Egorov property in perturbed cat maps*, *Journal of Physics A: Mathematical and Theoretical* **40** (2007), no. 32 9771–9781.
- [77] J. Ford, G. Mantica, and G. H. Ristow, *The Arnol’d cat: Failure of the correspondence principle*, *Physica D: Nonlinear Phenomena* **50** (1991), no. 3 493–520.
- [78] F. Benatti, H. Narnhofer, and G. L. Sewell, *A non-commutative version of the Arnold cat map*, *Letters in Mathematical Physics* **21** (1991), no. 2 157–172.
- [79] J. Andries, M. Fannes, P. Tuyls, and R. Alicki, *The dynamical entropy of the quantum Arnold cat map*, *Letters in Mathematical Physics* **35** (1995), no. 4 375–383.
- [80] A. W. Marshall, I. Olkin, and B. C. Arnold, *Inequalities: Theory of Majorization and Its Applications*. Springer Series in Statistics. Springer, New York, NY, 2011.